Cell Reports
Medicine

Report

Engineering human stem cell-derived islets to evade immune rejection and promote localized immune tolerance

Graphical abstract

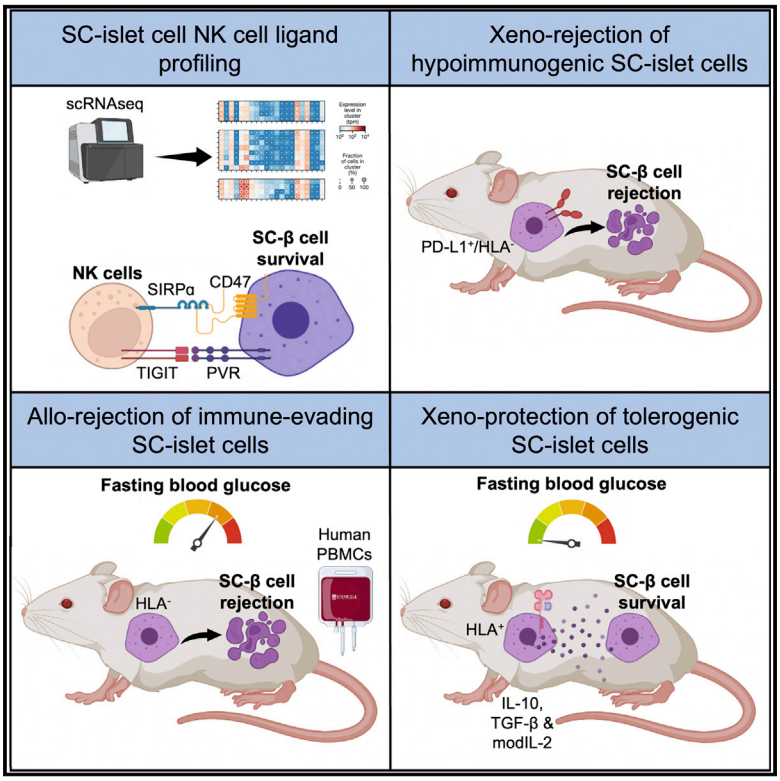

Highlights

- Stem cell-derived islets (SC-islets) possess an inhibitory NK cell ligand profile
- Immune-evasive SC-islets are rapidly rejected upon xeno-transplantation
- Immune-evasive SC-islets reverse diabetes and are slowly rejected in humanized mice
- Immune-tolerizing SC-islets reverse diabetes and resist xeno-rejection in NOD mice

Authors

Dario Gerace, Quan Zhou, Jennifer Hyoje-Ryu Kenty, ..., Kyle R. Boulanger, Hongfei Li, Douglas A. Melton

Correspondence

dmelton@harvard.edu

In brief

Currently, cell replacement therapy for type 1 diabetes is limited by the requirement for lifelong immunosuppression. Gerace et al. show that engineering stem cell-derived islets as vehicles of localized immune tolerance may be an approach to address this yet unanswered challenge.

Gerace et al., 2023, Cell Reports Medicine *4*, 100879
January 17, 2023
https://doi.org/10.1016/j.xcrm.2022.100879

CellPress

Cell Reports Medicine

CellPress
OPEN ACCESS

Report

Engineering human stem cell-derived islets to evade immune rejection and promote localized immune tolerance

Dario Gerace,[1,2] Quan Zhou,[1,2] Jennifer Hyoje-Ryu Kenty,[1] Adrian Veres,[1] Elad Sintov,[1] Xi Wang,[1] Kyle R. Boulanger,[1] Hongfei Li,[1] and Douglas A. Melton[1,3,*]

[1]Department of Stem Cell and Regenerative Biology, Harvard University, Howard Hughes Medical Institute, Harvard Stem Cell Institute, Boston, MA, USA

[2]These authors contributed equally

[3]Lead contact

*Correspondence: dmelton@harvard.edu

https://doi.org/10.1016/j.xcrm.2022.100879

SUMMARY

Immunological protection of transplanted stem cell-derived islet (SC-islet) cells is yet to be achieved without chronic immunosuppression or encapsulation. Existing genetic engineering approaches to produce immune-evasive SC-islet cells have so far shown variable results. Here, we show that targeting human leukocyte antigens (HLAs) and PD-L1 alone does not sufficiently protect SC-islet cells from xenograft (xeno)- or allograft (allo)-rejection. As an addition to these approaches, we genetically engineer SC-islet cells to secrete the cytokines interleukin-10 (IL-10), transforming growth factor β (TGF-β), and modified IL-2 such that they promote a tolerogenic local microenvironment by recruiting regulatory T cells (T_{regs}) to the islet grafts. Cytokine-secreting human SC-β cells resist xeno-rejection and correct diabetes for up to 8 weeks post-transplantation in non-obese diabetic (NOD) mice. Thus, genetically engineering human embryonic SCs (hESCs) to induce a tolerogenic local microenvironment represents a promising approach to provide SC-islet cells as a cell replacement therapy for diabetes without the requirement for encapsulation or immunosuppression.

INTRODUCTION

Type 1 diabetes (T1D) is an autoimmune disease that results in the destruction of the insulin-producing beta cells of the pancreas.[1] Cadaveric whole pancreas or islet transplantation are successful treatments for T1D; however, these are hampered by the limited number of donors and the requirement for lifelong immunosuppression.[2] To address the shortage of islet material, several protocols have been developed to steer the *in vitro* differentiation of human induced pluripotent stem cells (iPSCs) into functional stem cell-derived islets (SC-islets) that include glucose-response beta cells.[3–9]

Current strategies to protect allografted islet cells include systemic immunosuppression to modify the patient's immune system[10,11] and encapsulation.[12,13] More recently, genetic engineering of SC-islets to evade immune recognition has been attempted.[14–16] While this is a promising alternative, current engineering strategies are limited by transgene silencing and recurrent immune rejection.[17–19] Here, we generated immune-evasive SC-islet cells that over-express PD-L1 and the human leukocyte antigen (HLA)-E long-chain fusion from the constitutively expressed GAPDH locus in both HLA-competent and -deficient settings.[20,21] We also evaluated the induction of localized immune tolerance as a strategy to protect SC-islets. To achieve this, we engineered SC-islets to secrete a combination of tolerogenic cytokines including the interleukin-2 (IL-2) mutein (N88D),[22,23] IL-10, and transforming growth factor β (TGF-β).[24] Remarkably, immune-tolerizing SC-islets normalized hyperglycemia and provided protection from xenograft (xeno) rejection for up to 8 weeks after transplantation in non-obese diabetic (NOD) mice. Thus, immune-tolerizing SC-islet cells represent another step forward in providing a source of islets for the treatment of T1D with the long-term aim of eliminating the need for encapsulation or systemic immunosuppression.

RESULTS

Engineering immune-evasive SC-islet cells

Since GAPDH is constitutively expressed in all cells of the human islet (Figures S1A and S1B), we targeted the expression of PD-L1 and the HLA-E long-chain fusion to the GAPDH locus of human embryonic SCs (hESCs) and used luminescence as a reporter of cell viability. We chose to over-express PD-L1 as it was previously shown to protect SC-islet cells from xeno-rejection,[15] while the HLA-E long-chain fusion inhibits natural killer (NK) cells in an HLA-deficient context.[25–28] GAPDH-targeting plasmids were modified to include PD-L1 or HLA-E (Figures S1C–S1E) and used to create five hESC lines (Figure 1A): wild type (WT), HLA-deficient ($B2M^{-/-}$), PD-L1-expressing (PD-L1), HLA-deficient/PD-L1-expressing (B2P), and HLA-deficient/HLA-E-expressing

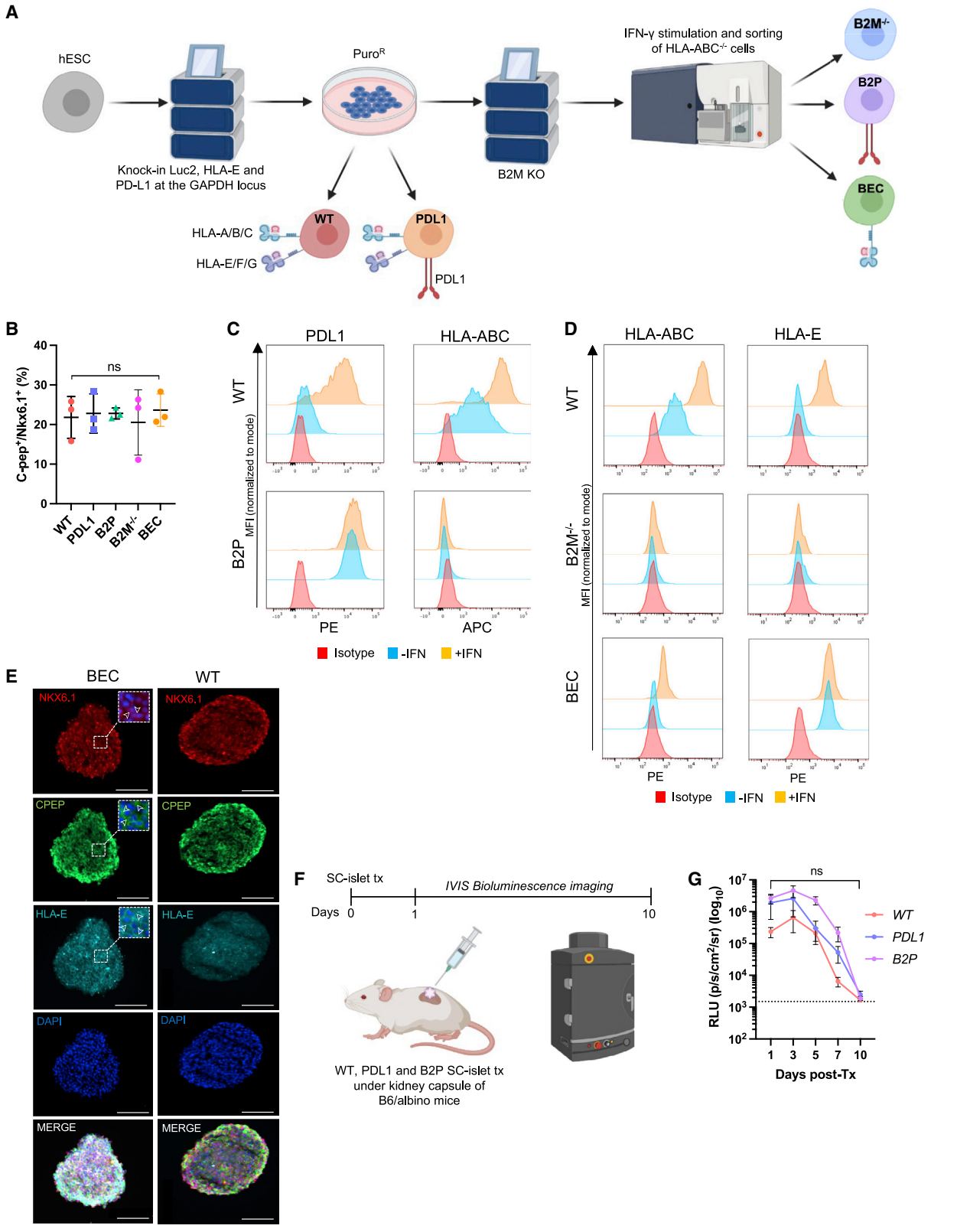

(legend on next page)

(BEC). All five gene-modified hESC lines successfully differentiated into Nkx6.1$^+$/C-peptide$^+$ SC-β cells as assessed by flow cytometry (Figures 1B and S1F). After interferon γ (IFN-γ) stimulation, HLA class I and PD-L1 were upregulated in WT SC-islet cells,[29] whereas B2P SC-islet cells constitutively over-expressed PD-L1 and lacked HLA class I expression (Figures 1C and S1G). A similar expression profile of HLA-E and HLA class I expression was observed in WT and BEC SC-islet cells (Figure 1D), with immunohistochemistry confirming the membrane localization of HLA-E on SC-β cells (Figure 1E).[28]

To confirm that human PD-L1 expressed on the surface of SC-islet cells binds PD-1, we assessed binding of fluorescently labeled, soluble human and mouse PD-1-Fc on WT and B2P SC-islet cells (Figure S1H). Both soluble human and mouse PD-1 bind membrane-bound PD-L1 on B2P SC-islet cells, whereas WT SC-islet cells do not endogenously express sufficient levels of PD-L1 to detectably bind human or mouse PD-1. We also observed a decrease in the binding affinity of soluble mouse PD-1 to human PD-L1.[30] We then transplanted WT, PD-L1, and B2P SC-islet cells under the kidney capsule of B6/albino mice to assess their ability to survive against xeno-rejection (Figure 1F), which had been previously demonstrated.[15] We used bioluminescence imaging to track SC-islet cell survival and found that all gene-modified SC-islet cells were rejected within 10 days after transplantation (Figure 1G). These results suggest that PD-L1 over-expression is not sufficient to protect HUES8-derived SC-islet cells from xeno-rejection and that the additional ablation of HLA expression does not improve xenograft survival in our *in vivo* model.

HLA-deficient SC-islet cells are resistant to allogeneic immune cell destruction

Since xeno-rejection does not mimic allograft (allo) rejection, we next chose to assess the survival of our HLA engineered SC-islet cells in an allogeneic setting. In concordance with previous studies,[31] we found that NK cells and CD4$^+$ and CD8$^+$ T cells represented ∼8%, 35%, and 10% of enriched peripheral blood mononuclear cells (PBMCs), respectively (Figures S2A and S2B). We then co-cultured IFN-γ-treated SC-islet cells with human PBMCs *in vitro* and showed that B2M$^{-/-}$ and BEC SC-islet cells possess significantly improved survival compared with WT (Figures 2A and 2B). HLA-E over-expression did not provide additional protective benefit. Additionally, similar survival patterns were observed when SC-islet cells were co-cultured with purified CD8$^+$ and CD4$^+$ T cells (Figures S2C–S2F). In all co-culture assays, there was no significant difference in the survival of all gene-modified SC-islet cells cultured with CD3/CD28 activated cells.

Since expression of T cell co-activating and co-inhibitory ligands dictates T cell function and is regulated by various stimuli including IFN-γ stimulation,[32] we performed bulk RNA sequencing on IFN-γ-stimulated WT CD49a$^+$ SC-β cells and assessed T cell ligand expression (Figure 2C). As expected, IFN-γ stimulation upregulated expression of the T cell co-inhibitory ligands *PD-L1* and *LGALS9* (galectin 9) in SC-β cells (Figure 2D).[33,34] Conversely, while we did not detect transcripts for many T cell co-activating ligands other than HLA genes, we found that IFN-γ stimulation upregulated members of the tumor necrosis factor (TNF) receptor superfamily *HVEM* and *CD40* and the major histocompatibility complex (MHC)-associated gene butyrophilin subfamily 3 member A1 (*BNT3A1*) (Figure 2E).[35–37] These results suggest that in the absence of classical HLA-TCR signaling due to HLA knockout, other co-stimulatory and co-inhibitory T cell ligands are expressed in SC-β cells that may influence T cell function.

HLA-deficient SC-islet cells are resistant to allogeneic NK cell destruction

We next assessed the effect of HLA deletion and HLA-E over-expression on NK cell function against SC-islet cells. When co-cultured with NK-92 MI cells, BEC SC-islet cells showed no significant difference in survival compared with WT SC-islet cells, whereas HLA-deficient SC-islet cells were susceptible to NK-92 MI cytotoxicity (Figure S3A).[28] The strong protective effect of HLA-E against NK-92 MI cells is likely due to the high percentage (∼96.1%) of NKG2A$^+$/NKG2C$^-$ cells (Figure S3B), which biases NK cell inhibition.

While NK cell lines are useful tools for assessing NK cell cytotoxicity, they do not accurately recapitulate primary NK cell receptor expression and function. Previous studies have shown that in the absence of IL-2 activation, human NK cells do not destroy HLA-deficient endothelial cells and platelets.[38,39] Thus, prior to co-culture with gene-modified SC-islet cells, we pre-activated human NK cells with IL-2 for 5 days as previously described.[38] Enriched NK cells consisted of ∼80% CD56^{dim} and ∼5% CD56^{high} NK cells (Figures S3C and S3D). Surprisingly, despite IL-2 pre-activation, we observed no significant difference in survival between gene-modified SC-islet cells (Figure 2F). Since HLA-E over-expression does not provide any additional protective benefit to HLA-deficient SC-islet cells against NK cell cytotoxicity, we chose to interrogate WT and B2M$^{-/-}$ SC-islet cells moving forward. We assessed the survival of WT and

Figure 1. Generation of immune-evasive SC-islet cells

(A) Schematic of the genetic engineering strategy to generate immune-evasive hESCs.

(B) Analysis of Nkx6.1$^+$/C-peptide$^+$ SC-β cells (S6d14). Data are presented as mean ± SD (n = 3 independent differentiations). p values were determined by one-way ANOVA, *p < 0.05.

(C) PD-L1 and HLA-ABC expression on SC-β cells. Data are presented as mean fluorescence intensity (MFI) normalized to mode.

(D) HLA-ABC and HLA-E expression on SC-β cells. Data are presented as MFI normalized to mode.

(E) Immunofluorescence staining of CD49a$^+$-enriched SC-β cells (S6d14). White arrowheads highlight expression of Nkx6.1, C-peptide, and HLA-E, respectively. Scale bars: 100 μm.

(F) Schematic of *in vivo* SC-islet cell xeno-rejection model.

(G) Analysis of xenograft rejection. Data are presented as mean ± SEM (n = 5/group). p values were determined by two-way ANOVA between groups, *p < 0.05. Dashed line represents background luminescence.

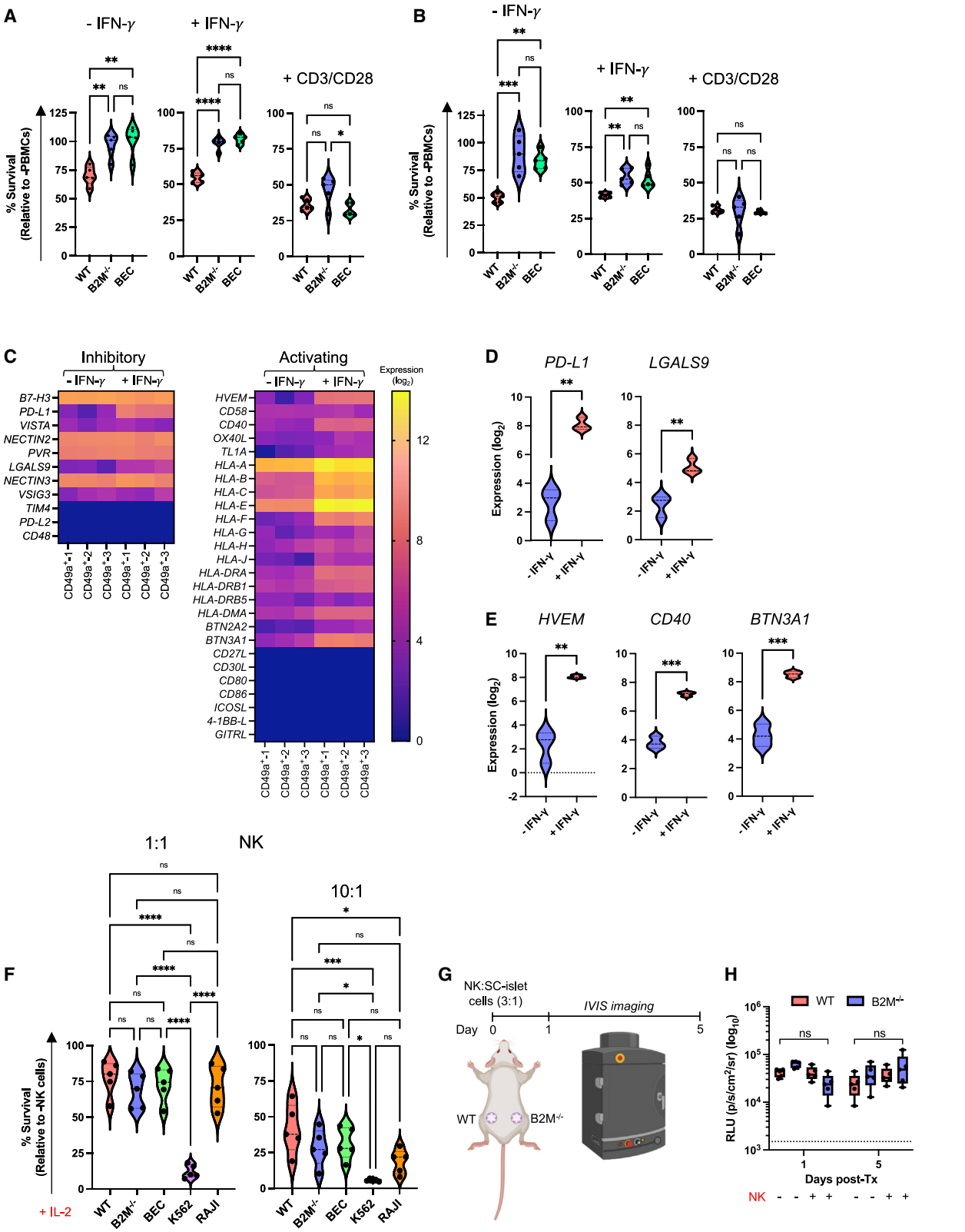

(legend on next page)

B2M$^{-/-}$ SC-islet cells after transplantation with IL-2 pre-activated NK cells in Scid/beige mice (Figure 2G). Again, there was no significant difference in WT and B2M$^{-/-}$ SC-islet cell survival *in vivo* (Figures 2H and S3E). Taken together, these results suggest that HLA-deficient SC-islet cells are intrinsically resistant to NK cell cytotoxicity and that their survival *in vitro* is recapitulated *in vivo*.

SC-β cells possess an NK cell evasive ligand phenotype

Since we expected B2M$^{-/-}$ SC-islet cells to be susceptible to IL-2 pre-activated NK cells,[38] and considering NK cell function is dictated by a balance of inhibitory and activating signals, we hypothesized that the endogenous ligand receptor profile of SC-β cells may be conducive to an NK cell evasive phenotype. We therefore re-analyzed single-cell RNA sequencing (scRNA-seq) expression datasets from our existing *in vitro* SC-β cell differentiation,[7] an *in vivo* SC-β cell transplantation,[40] and primary human islets,[41] focusing on the expression of NK cell ligands. We found that SC-β cells intrinsically lack expression of many non-HLA NK cell activating ligands such as *NCR3LG1*, *MICA*, *MICB*, *UBLP1*, *ULBP2*, *CD48*, and *CD72*, while they do express many non-HLA inhibitory ligands such as *PVR*, *CD47*, *CDH2*, *NECTIN1*, *NECTIN2*, and *NECTIN3* (Figure 3A). Importantly, the expression of non-HLA ligands does not change in SC-β cells after transplantation. However, in contrast, HLA expression increased after transplantation almost exclusively in SC-α cells, except for *HLA-E*, which also increased in SC-β and SC-enterochromaffin cells. Furthermore, while the expression of non-HLA NK cell ligands in *in vitro* differentiated and 6-month post-transplantation SC-islets is like that in primary human islets, SC-islets remain somewhat less immunogenic.[42] We then compared the expression of non-HLA ligands at the surface of WT and B2M$^{-/-}$ SC-β cells by flow cytometry and showed that HLA deletion does not alter their expression (Figure 3B).

While scRNA-seq and flow cytometry suggests that SC-β cells possess a diminished NK cell activating ligand phenotype, we chose to confirm this by comparing the expression of NK cell ligands on SC-β cells and endothelial cells. This is because it had been shown that HLA-deficient endothelial cells are susceptible to IL-2 pre-activated NK cells,[38] and we hypothesized that the susceptibility to NK cell cytotoxicity may be due to the expression of activating ligands. Thus, we differentiated WT and B2M$^{-/-}$ hESCs into SC-endothelial cells and assessed differentiation efficiency by flow cytometry, which showed >95% CD31^{+} SC-endothelial cells derived from both cell lines (Figures S4A and S4B). A flow cytometric comparison of NK cell ligand expression on SC-β and SC-endothelial cells showed that the MIC and ULBP proteins were expressed in SC-endothelial cells, whilst they were either absent or less expressed on SC-β cells (Figures S4C and S4D). Next, we sought to understand how the expression of NK cell ligands is regulated by a partial pro-inflammatory stimulus. We performed bulk RNA-seq of IFN-γ-treated SC-β and SC-endothelial cells and found that the expression of most NK cell ligands is not IFN-γ regulated, except for the HLA molecules (Figure S4E). Thus, within an HLA-deficient context, the expression of non-HLA NK cell ligands is stable upon inflammatory stimulus.

To identify potential ligand-receptor pathways that may result in the survival of B2M$^{-/-}$ SC-islet cells when co-cultured with IL-2 pre-activated NK cells, we assessed the surface expression of NK cell activating and inhibitory receptors on freshly isolated and IL-2 pre-activated NK cells. In general, we found that the expression of the activating receptors NKp30, NKp46, DNAM-1, and NKG2D were upregulated upon IL-2 pre-activation in both CD56^{dim} and CD56^{high} NK cells, whereas NKp80 was downregulated (Figure 3C).[43] Similarly, since we observed surface expression of the inhibitory ligands CD47, PVR, and the cadherins and nectins on SC-β cells, we assessed the expression of their cognate receptors SIRPα, TIGIT, KLRG1, and CD96, respectively, on NK cells. As reported by Deuse et al.,[38] we observed significant upregulation of SIRPα on IL-2 pre-activated NK cells (Figure 3D). Additionally, TIGIT and CD96 were upregulated after IL-2 pre-activation. Next, we hypothesized that the CD47-SIRPα and PVR-TIGIT ligand-receptor pathways may be involved in the NK cell evasive phenotype of B2M$^{-/-}$ SC-islet cells. When B2M$^{-/-}$ SC-islet cells were co-cultured with pre-activated NK cells in the presence of anti-SIRPα and anti-TIGIT neutralizing antibodies, SC-islet cell survival decreased (Figure 3E). Taken together, these data suggest that SC-β cells intrinsically possess and sustain a diminished NK cell activating ligand profile and that this ligand phenotype may explain their resistance to IL-2 pre-activated NK cell cytotoxicity.

HLA-deficient SC-islet cells demonstrate delayed graft rejection and reverse diabetes in humanized mice

Having demonstrated that HLA-deficient SC-islet cells resist PBMC cytotoxicity *in vitro* and NK cell cytotoxicity *in vitro* and *in vivo*, we assessed the ability of HLA-deficient SC-islet cells to normalize hyperglycema in diabetic, NSG double knockout (DKO) mice prior to PBMC injection (Figure 3F). By 10 weeks post-transplantation, there was no significant difference in blood glucose levels of mice transplanted with WT

Figure 2. *In vitro* co-culture of immune-evasive SC-islet cells with allogeneic human immune cells

(A and B) SC-islet cell survival when co-cultured with primary human PBMCs at 1:1 and 3:1 PBMC/SC-islet ratio. Data are presented as mean ± SD (n = 5 donors in technical triplicate). p values were determined by one-way ANOVA with Tukey's post-hoc test, *p < 0.05.

(C) T cell ligand gene expression in IFN-γ-treated CD49a^{+} SC-β cells. Ligand expression is presented as fold change (log_2).

(D and E) Differential expression of T cell co-inhibitory and co-activating ligands in IFN-γ-treated CD49a^{+} SC-β cells. Ligand expression is presented as fold-change (log_2). p values were determined by Student's t test.

(F) SC-β cell survival when co-cultured with primary human CD56^{+} NK cells at 1:1 and 10:1 NK:SC-β cell ratios. Data are presented as mean ± SD (n = 5 donors in technical triplicate). p values were determined by one-way ANOVA with Tukey's post-hoc test, *p < 0.05.

(G) Schematic of *in vivo* NK cell cytotoxicity assay.

(H) Analysis of *in vivo* NK cell assay. NK and SC-islet cell mixtures (3:1) were transplanted subcutaneously in Scid/beige mice (n = 5/group), and all were monitored by bioluminescence imaging on days 1 and 5 post-transplantation. Data are presented as mean ± SEM. p values were determined by two-way ANOVA, *p < 0.05. Dashed line represents background luminescence.

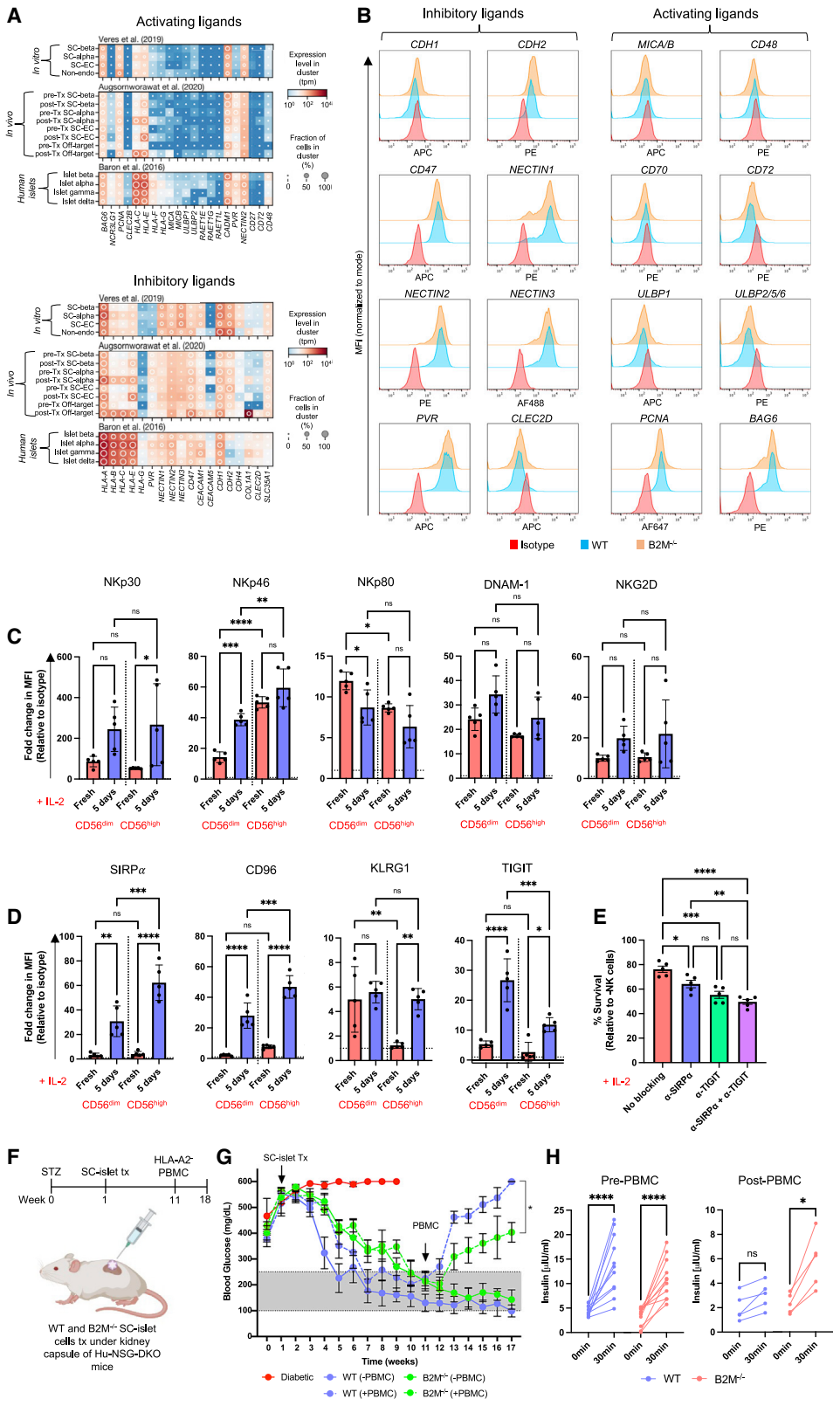

(legend on next page)

and B2M$^{-/-}$ SC-islet cells (Figure 3G). Once blood glucose levels had been normalized, we injected HLA-A2^{-} (mismatched) PBMCs and assessed allo-rejection by monitoring blood glucose levels. WT SC-islet cells were destroyed within 2 weeks, whereas the rejection of B2M$^{-/-}$ SC-islet cells was delayed. At 7 weeks post-PBMC injection, *in vivo* glucose-stimulated insulin secretion (GSIS) assay showed that animals transplanted with WT SC-islet cells lost *in vivo* graft function, while some graft function was observed in animals transplanted with B2M$^{-/-}$ SC-islet cells (Figure 3H). These results suggest that B2M$^{-/-}$ SC-islet cells reverse diabetes and demonstrate delayed allo-rejection; however, it is likely that they would ultimately be completely rejected.

Cytokine-secreting SC-β cells are protected from xeno-rejection and reverse diabetes in NOD mice

As a result of the varying success of immune-evasive engineering to protect SC-islet cells, we pursued a complementary strategy by engineering SC-islet cells to secrete the cytokines IL-2 mutein, TGF-β, and IL-10 as vehicles of localized immune tolerance. The IL-2 mutein (N88D) possesses reduced affinity for the IL-2Rβγ receptor, resulting in the production of a regulatory T cell (T_{reg})-selective molecule that preferentially expands T_{regs} while having a minimal effect on CD4^{+} and CD8^{+} memory T cells.[22,23] Since the immune-suppressive phenotype of T_{regs} requires IL-10 and TGF-β, we included these two cytokines in our immune-tolerizing approach.[24] Consequently, we engineered human pluripotent stem cells to express modified IL-2, IL-10, and TGF-β from the GAPDH locus (Figure 4A). Differentiation of this genetically modified cell line, called 2B10, resulted in ~30% Nkx6.1^{+}/C-peptide^{+} SC-β cells as assessed by flow cytometry (Figure 4B). When stimulated with sequential low- and high-glucose challenges in an *in vitro* GSIS assay, 2B10 SC-islet cells demonstrated a similar insulin secretion profile as WT and significantly upregulated insulin secretion in response to glucose stimulation (Figure 4C). We also confirmed that 2B10 SC-islet cells secrete modified IL-2, TGF-β, and IL-10 and that the amount of cytokine secreted was SC-islet-cell-concentration dependent (Figure S4F). We next sought to determine if cytokine-secreting SC-islet cells were protected from allogeneic human PBMC destruction *in vitro*. When WT and 2B10 SC-islet cells were co-cultured with human PBMCs *in vitro*, 2B10 SC-islet cells showed significantly improved survival compared with their WT counterparts (Figure 4D).

Because humanized mice bias the engraftment of CD3^{+} T cells,[44] we chose to assess the survival of cytokine-secreting SC-islet cells in a xenogeneic mouse model. When 2B10 SC-islet cells were transplanted in B6/albino mice, they survived up to 9 weeks post-transplantation, while WT SC-islet cells were destroyed within 2 weeks (Figures 4E and S4G). We also found that WT grafts contained little to no remaining SC-islet cells, while 2B10 grafts contained surviving insulin-producing cells and T_{regs} localized within the graft (Figure 4F). Finally, to demonstrate that cytokine-secreting SC-islet cells can survive xeno-rejection and reverse diabetes, we transplanted CD49a^{+} SC-β cells in autoimmune diabetic NOD mice (Figures 4G and 4H). We found that WT SC-β cells temporarily survive and reverse diabetes for 2–3 weeks. Excitingly, 2B10 SC-β cells reversed diabetes for the period of the experiment (8 weeks) in the absence of any xeno-rejection. Collectively, these data suggest that SC-islet cells can be engineered to co-secrete immune-modulatory cytokines that induce a tolerogenic local microenvironment characterized by T_{reg} infiltration that sustains xenograft survival while also reversing autoimmune diabetes in NOD mice.

DISCUSSION

The utility of an immune-evasive/-tolerogenic islet cell replacement therapy relies on the ability to maintain transgene expression throughout cell differentiation and after transplantation. Here, we showed that engineering SC-islet cells to constitutively express tolerogenic molecules from the *GAPDH* locus resulted in persistent transgene expression. In contrast to a study by Yoshihara et al.,[15] we also report the lack of a xeno-protective effect of PD-L1 over-expression in HUES8-derived SC-islet cells. This may be explained by species-specific differences in PD-L1/PD-1 binding.[45,46] In fact, we observed decreased binding of soluble mouse PD-1 to human PD-L1 expressed on SC-islet cells. We also cannot exclude the possibility that the level of PD-L1 expression driven by the endogenous GAPDH promoter (~50-fold increase) is not sufficient to provide immune protection. While our results suggest that over-expression of human PD-L1 is not sufficient to overcome xeno-rejection in our model, this strategy may still be useful in an allogeneic setting.

Diminishing the immune recognition of SC-islet cells by manipulating the expression of HLA molecules has also shown some promise as a potential immune-protective strategy.[14] Thus, we chose to assess a universal HLA engineering strategy

Figure 3. SC-islet cell NK cell ligand profile

(A) NK cell ligand expression in pre- and post-transplant SC-β cells and primary human islet cells. The shading displays mean expression as *z*-normalized transcripts per million mapped reads (*z*-norm, TPMs), and diameter denotes fractional expression.

(B) NK cell ligand expression on SC-β cells. Data are presented as MFI normalized to mode and are representative of three independent experiments.

(C and D) Analysis of NK cell activating and inhibitory receptor expression. Data are presented as mean fold change in MFI ±SD (n = 5 donors) normalized to isotype control (dashed line). p values were determined by two-way ANOVA, *p < 0.05.

(E) NK cell receptor antibody blocking assay. Data are presented as mean ± SD (n = 5 donors in technical triplicate). p values were determined by one-way ANOVA with Tukey's post-hoc test, *p < 0.05.

(F) Schematic of SC-islet cell transplantation in diabetic, humanized mice.

(G) Non-fasting blood glucose concentrations after SC-islet transplantation in humanized mice. At week 10, each group of mice was divided, and half were humanized by intraperitoneal (i.p.) injection of 5 × 10^{7} HLA-A2^{-} human PBMCs. Data are presented as mean ± SD (n = 12/group). p values were determined by two-way ANOVA, *p < 0.05.

(H) *In vivo* GSIS pre- and 7 weeks post-humanization. Plasma insulin concentration was measured t = 0 and 30 min after glucose injection. Data are represented as mean ± SD (n = 5/group). p values were determined by unpaired t test, *p < 0.05.

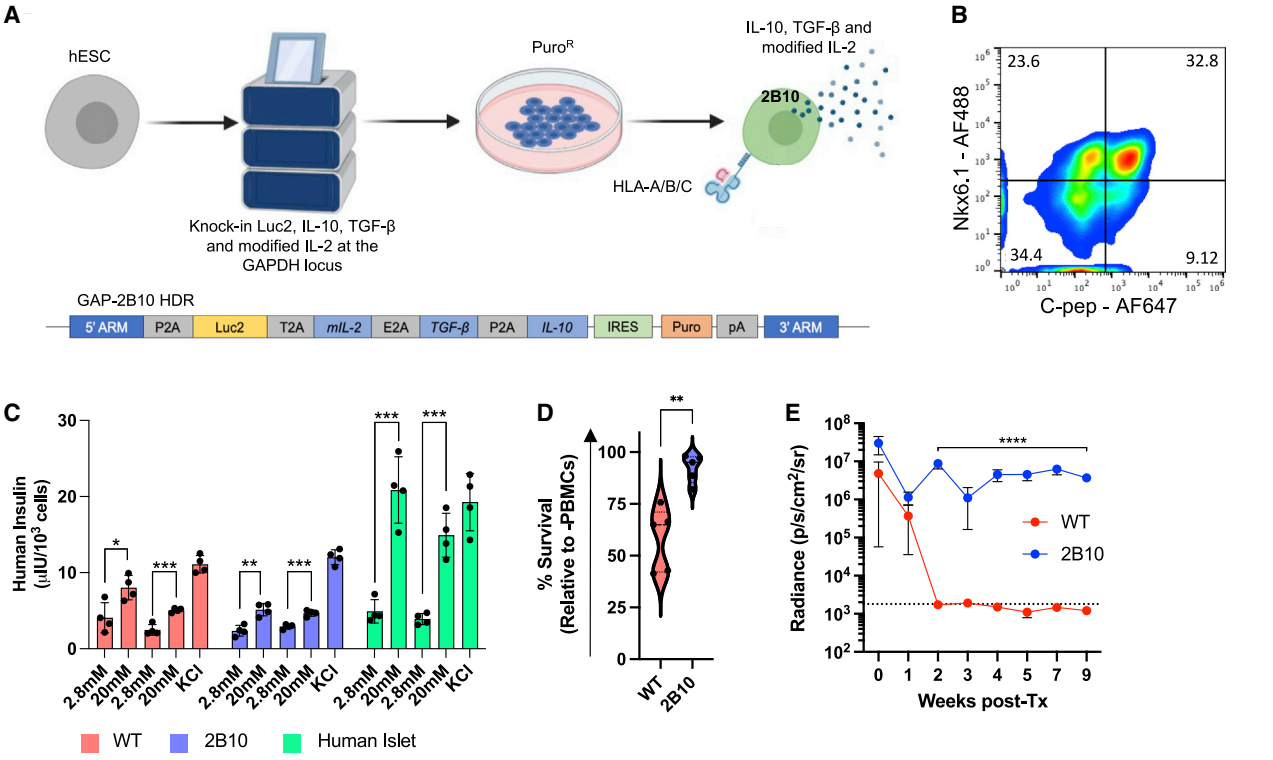

(legend on next page)

that would potentially allow for transplantation of SC-islets in any diabetic individual regardless of HLA type.[28] In concordance with previous studies, HLA-deficient SC-islet cells were resistant to PBMC cytotoxicity *in vitro*.[47,48] We also found that SC-β cells modulate their T cell ligand profile in response to partial inflammatory stimulus. Analysis of T cell ligand transcripts in SC-β cells suggests that exploiting the LGALS9/TIM-3 signaling axis may be of interest. In fact, like *PD-L1*, *LGALS9* is frequently upregulated in cancer cells, where it contributes to tumor progression by inhibition of T cell function.[49,50] The T cell activating ligands *HVEM*, *CD40*, and *BTN3A1* are potential targets to knock out in SC-islet cells to further influence T cell function.

We also showed that HLA-deficient SC-islet cells are resistant to pre-activated NK cell cytotoxicity both *in vitro* and *in vivo*. This may be due to the lack of expression of NK cell activating ligands such as the MIC and ULBP proteins on SC-β cells. While treatment with IFN-γ did not alter the expression of non-HLA NK cell ligands on SC-β cells, other pro-inflammatory cytokines have been shown to regulate the expression of anti-viral and immune-associated genes in mouse islets.[51] This observation may also extend to NK cell ligand expression, which would potentially alter the immunogenicity of SC-islet cells. However, since many immunodeficient mouse models lack critical components for NK cell survival and function such as SIRPα and IL-15,[52] they do not support long-term engraftment of human NK cells, and we cannot exclude the possibility of HLA-deficient SC-islet cell destruction in a mouse model that better supports NK cell engraftment. Furthermore, while the transplantation of HLA-deficient SC-islet cells was able to normalize blood glucose levels in diabetic mice, after humanization, the cells were eventually destroyed with delayed rejection kinetics. This could be explained by the presence of other human immune cell subsets such as macrophages, monocytes, and dendritic cells that may play a role in indirect allo-rejection.[53–55] Ultimately, this highlights the limitations of exclusively using *in vitro* immune cell co-culture assays to assess the effect of genetic modification on the protection of SC-islet cells from immune destruction.[29,48]

Finally, we show for the first time that SC-islet cells engineered to secrete modified IL-2, TGF-β, and IL-10 are protected against xeno-rejection and reverse autoimmune diabetes in NOD mice. This combination of cytokines resulted in the localization of T_{regs} within the SC-islet grafts, providing localized immune tolerance and sustained survival of the SC-islets. Similarly, several studies have attempted to induce localized immune tolerance of SC-islet grafts by engineering chimeric antigen receptor (CAR)-T_{regs} to recognize cell-type-specific antigens such that they migrate toward the grafted cells and protect them from immune rejection.[56–58] However, while these studies demonstrate the potential utility of *ex-vivo*-engineered T_{regs} for protection against allo-rejection, the phenotypic stability of these cells is poorly understood, and patients would likely require repeated treatments to sustain immune tolerance. Thus, our unique approach of using SC-islet grafts to induce localized immune tolerance has several important implications. First, since β cells are professional secretory cells with a significant translatory demand, it demonstrates that SC-islet cells can be co-opted to secrete other proteins while maintaining their designed function.[59] Second, the intrinsic ligand profile of the desired cell type should be considered when determining the set of genetic modifications required to generate immune-evasive cells, as some cell types may not require extensive genetic manipulation. Third, our results provide validation for the use of immune-tolerizing approaches (either alone or in conjunction with immune evasion) as a method to protect SC-islet cells from the immune system. A variation of this approach may be to include some, but not all, cells in the transplant that secrete these tolerizing molecules. Similarly, accessory cells that intrinsically possess immune-modulatory functions could also be included within the designer islets.[60] Overall, our approach may eliminate the need for encapsulation or immunosuppression, a long-standing goal of the islet transplantation field.

Limitations of the study

Although HLA-deficient SC-islet cells possessed improved survival in *in vitro* PBMC co-culture assays (Figures 2A and 2B), we found that these results did not translate *in vivo*. Choosing an appropriate humanized mouse model is essential to evaluate immune-evasion/-tolerizing genetic engineering strategies. Many PBMC humanized mouse models such as that used in this study do not fully recapitulate human allo-rejection since they bias $CD3^+$ cell engraftment and lack other immune cell subsets. Thus, while HLA-deficient SC-islets demonstrated delayed rejection in the PBMC humanized mouse model (Figure 3G), we cannot exclude the possibility that in $CD34^+$ or BLT mice (humanized mouse models that better recapitulate human immune components) these cells would be rejected earlier. For these reasons, validating the protective effect of immune-evasion/-tolerizing genetic engineering strategies should be conducted in humanized mouse models that more accurately reflect allo-rejection and recapitulate human T1D.

In this study, we ultimately chose to use the NOD mouse as a xeno-rejection model to evaluate our immune-tolerizing strategy

Figure 4. Immune-tolerizing SC-islet cells survive xeno-rejection

(A) Schematic of the genetic engineering strategy to generate immune-tolerizing hESCs.

(B) Analysis of Nkx6.1$^+$/C-peptide$^+$ SC-β cells derived from immune-tolerizing hESCs (S6d8).

(C) *In vitro* GSIS. WT (red), 2B10 (blue) SC-islets, and primary human islets (green) were challenged with consecutive low (2.8 mM) and high (20 mM) glucose stimulations, followed by depolarization with 30 mM KCl. Data are represented as mean ± SD (n = 4). p values were determined by unpaired t test, *p < 0.05.

(D) SC-islet cell survival when co-cultured with primary human PBMCs at a 1:1 ratio. Data are presented as mean ± SD (n = 5 donors in technical triplicate). p values were determined by Student's t test.

(E) Analysis of *in vivo* graft survival in B6/albino mice. Data are presented as mean ± SD (n = 4/group). p values were determined by two-way ANOVA, *p < 0.05.

(F) Immunostaining of SC-islet grafts showing presence of INS$^+$ cells and T_{reg} recruitment at 5 weeks post-transplantation. Scale bars: 100 μm.

(G) Schematic of cytokine-secreting SC-β cell transplantation in diabetic NOD mice.

(H) Non-fasting blood glucose concentrations after SC-β cell transplantation in NOD mice. Data are presented as mean ± SD (n = 3/group). p values were determined by two-way ANOVA, *p < 0.05.

as it is an autoimmune model of diabetes and does not possess the immune cell bias of humanized mouse models. However, by using such a strong model of graft rejection, additional immune barriers are introduced that require complex genetic engineering approaches as a solution. This means combining gene knockouts and knockins to generate the desired immune-evasive/-tolerizing cell product. Knockin of multiple genes at a specific locus in the genome requires large homology directed repair templates, which is associated with poor integration efficiency and recovery of genetically unstable clones. Exploring the possibility of introducing tolerogenic molecules at multiple constitutively expressed loci could reduce the size of homology-directed repair (HDR) templates and result in the recovery of genetically stable homozygous knockin clones. Striking a balance between HDR length and the number of editing events may permit the introduction of more foreign genetic material into the genome without destabilizing effects.

Furthermore, since immune-tolerizing SC-islets secrete cytokines from all cells within the islet, there is a risk that the concentration of constitutively secreted cytokines may result in chronic immunosuppression. Thus, it is important to evaluate the immune status of mice receiving immune-tolerizing SC-islet cells as chronic immunosuppression should be avoided. This could have been partially evaluated by titrating the concentration of the individual cytokines *in vitro* with human PBMCs and conducting a high-resolution analysis of the composition of immune cells and their resulting phenotypes. However, if transplantation of immune-tolerizing SC-islets does result in chronic immunosuppression, the ability to enrich for specific endocrine cell populations may allow us to adjust the dose of cytokine-secretion by generating designer islets composed of cytokine-secreting and non-cytokine-secreting endocrine cells such that localized graft tolerance is achieved.

STAR★METHODS

Detailed methods are provided in the online version of this paper and include the following:

SUPPLEMENTAL INFORMATION

Supplemental information can be found online at https://doi.org/10.1016/j.xcrm.2022.100879.

ACKNOWLEDGMENTS

D.A.M. is the Distinguished Research Fellow at Vertex Pharmaceuticals. This research was performed while D.A.M. was on the faculty at Harvard University. This work was supported by grants from the Harvard Stem Cell Institute (DP-0180-18-02), JDRF (5-COE-2020-967-M-N), and the JPB Foundation (award no. 1094). We would like to thank Ramona Pop for discussions on manuscript content. Some illustrations in the figures were made using BioRender.

AUTHOR CONTRIBUTIONS

Conceptualization, original hypothesis, and design of the study, D.G. and D.A.M.; methodology, D.G., Q.Z., J.H.-R.K., and D.A.M.; investigation, D.G., Q.Z., J.H.-R.K., A.V., E.S., X.W., K.R.B., H.L., and D.A.M.; writing – original draft, D.G.; writing – review & editing, all authors; resources, D.G., Q.Z., J.H.-R.K., and D.A.M.; supervision, D.G., Q.Z., J.H.-R.K., and D.A.M.

DECLARATION OF INTERESTS

D.G., Q.Z., and D.A.M. are named on US provisional patent application serial no. 63/340,453, which is related to this work. D.G. is an employee of Inventia Life Sciences. D.A.M. and Q.Z. are employees of Vertex Pharmaceuticals. These companies were not involved in any aspect of the work.

Received: April 11, 2022
Revised: September 2, 2022
Accepted: December 8, 2022
Published: January 3, 2023

REFERENCES

1. Atkinson, M.A., and Maclaren, N.K. (1994). The pathogenesis of insulin-dependent diabetes mellitus. N. Engl. J. Med. *331*, 1428–1436.
2. Shapiro, A.M.J., Ricordi, C., Hering, B.J., Auchincloss, H., Lindblad, R., Robertson, R.P., Secchi, A., Brendel, M.D., Berney, T., Brennan, D.C., et al. International trial of the Edmonton protocol for islet transplantation. N. Engl. J. Med. 2006; 355: 1318-1330.

3. Millman, J.R., Xie, C., Van Dervort, A., Gürtler, M., Pagliuca, F.W., and Melton, D.A. (2016). Generation of stem cell-derived beta-cells from patients with type 1 diabetes. Nat. Commun. *7*, 12379.

4. Nair, G.G., Liu, J.S., Russ, H.A., Tran, S., Saxton, M.S., Chen, R., et al. (2019). Recapitulating endocrine cell clustering in culture promotes maturation of human stem-cell-derived beta cells. Nat. Cell Biol. *21*, 263–274.

5. Pagliuca, F.W., Millman, J.R., Gürtler, M., Segel, M., Van Dervort, A., Ryu, J.H., et al. (2014). Generation of functional human pancreatic beta cells in vitro. Cell *159*, 428–439.

6. Rezania, A., Bruin, J.E., Arora, P., Rubin, A., Batushansky, I., Asadi, A., et al. (2014). Reversal of diabetes with insulin-producing cells derived in vitro from human pluripotent stem cells. Nat. Biotechnol. *32*, 1121–1133.

7. Veres, A., Faust, A.L., Bushnell, H.L., Engquist, E.N., Kenty, J.H.R., Harb, G., et al. (2019). Charting cellular identity during human in vitro beta-cell differentiation. Nature *569*, 368–373.

8. Russ, H.A., Parent, A.V., Ringler, J.J., Hennings, T.G., Nair, G.G., Shveygert, M., Guo, T., Puri, S., Haataja, L., Cirulli, V., et al. (2015). Controlled induction of human pancreatic progenitors produces functional beta-like cells in vitro. EMBO J. *34*, 1759–1772.

9. D'Amour, K.A., Bang, A.G., Eliazer, S., Kelly, O.G., Agulnick, A.D., Smart, N.G., Moorman, M.A., Kroon, E., Carpenter, M.K., and Baetge, E.E. (2006). Production of pancreatic hormone-expressing endocrine cells from human embryonic stem cells. Nat. Biotechnol. *24*, 1392–1401.

10. Hartemann, A., Bensimon, G., Payan, C.A., Jacqueminet, S., Bourron, O., Nicolas, N., Fonfrede, M., Rosenzwajg, M., Bernard, C., and Klatzmann, D. (2013). Low-dose interleukin 2 in patients with type 1 diabetes: a phase 1/2 randomised, double-blind, placebo-controlled trial. Lancet Diabetes Endocrinol. *1*, 295–305.

11. Herold, K.C., Bundy, B.N., Long, S.A., Bluestone, J.A., DiMeglio, L.A., Dufort, M.J., Gitelman, S.E., Gottlieb, P.A., Krischer, J.P., Linsley, P.S., et al. (2019). An anti-CD3 antibody, teplizumab, in relatives at risk for type 1 diabetes. N. Engl. J. Med. *381*, 603–613.

12. Alagpulinsa, D.A., Cao, J.J.L., Driscoll, R.K., Sîrbulescu, R.F., Penson, M.F.E., Sremac, M., Engquist, E.N., Brauns, T.A., Markmann, J.F., Melton, D.A., and Poznansky, M.C. (2019). Alginate-microencapsulation of human stem cell-derived β cells with CXCL12 prolongs their survival and function in immunocompetent mice without systemic immunosuppression. Am. J. Transplant. *19*, 1930–1940.

13. Bochenek, M.A., Veiseh, O., Vegas, A.J., McGarrigle, J.J., Qi, M., Marchese, E., Omami, M., Doloff, J.C., Mendoza-Elias, J., Nourmohammadzadeh, M., et al. (2018). Alginate encapsulation as long-term immune protection of allogeneic pancreatic islet cells transplanted into the omental bursa of macaques. Nat. Biomed. Eng. *2*, 810–821.

14. Parent, A.V., Faleo, G., Chavez, J., Saxton, M., Berrios, D.I., Kerper, N.R., Tang, Q., and Hebrok, M. (2021). Selective deletion of human leukocyte antigens protects stem cell-derived islets from immune rejection. Cell Rep. *36*, 109538.

15. Yoshihara, E., O'Connor, C., Gasser, E., Wei, Z., Oh, T.G., Tseng, T.W., Wang, D., Cayabyab, F., Dai, Y., Yu, R.T., et al. (2020). Immune-evasive human islet-like organoids ameliorate diabetes. Nature *586*, 606–611.

16. Sintov, E., Nikolskiy, I., Barrera, V., Hyoje-Ryu Kenty, J., Atkin, A.S., Gerace, D., Ho Sui, S.J., Boulanger, K., and Melton, D.A. (2022). Whole-genome CRISPR screening identifies genetic manipulations to reduce immune rejection of stem cell-derived islets. Stem Cell Rep. *17*, 1976–1990.

17. Monti, P., Scirpoli, M., Maffi, P., Ghidoli, N., De Taddeo, F., Bertuzzi, F., Piemonti, L., Falcone, M., Secchi, A., and Bonifacio, E. (2008). Islet transplantation in patients with autoimmune diabetes induces homeostatic cytokines that expand autoreactive memory T cells. J. Clin. Invest. *118*, 1806–1814.

18. Stegall, M.D., Lafferty, K.J., Kam, I., and Gill, R.G. (1996). Evidence of recurrent autoimmunity in human allogeneic islet transplantation. Transplantation *61*, 1272–1274.

19. Abou-Daya, K.I., Tieu, R., Zhao, D., Rammal, R., Sacirbegovic, F., Williams, A.L., Shlomchik, W.D., Oberbarnscheidt, M.H., and Lakkis, F.G. (2021). Resident memory T cells form during persistent antigen exposure leading to allograft rejection. Sci. Immunol. *6*, eabc8122.

20. Gerace, D., Boulanger, K.R., Hyoje-Ryu Kenty, J., and Melton, D.A. (2021). Generation of a heterozygous GAPDH-Luciferase human ESC line (HVRDe008-A-1) for in vivo monitoring of stem cells and their differentiated progeny. Stem Cell Res. *53*, 102371.

21. Sintov, E., Gerace, D., and Melton, D.A. (2021). A human ESC line for efficient CRISPR editing of pluripotent stem cells. Stem Cell Res. *57*, 102591.

22. Peterson, L.B., Bell, C.J.M., Howlett, S.K., Pekalski, M.L., Brady, K., Hinton, H., Sauter, D., Todd, J.A., Umana, P., Ast, O., et al. (2018). A long-lived IL-2 mutein that selectively activates and expands regulatory T cells as a therapy for autoimmune disease. J. Autoimmun. *95*, 1–14.

23. Khoryati, L., Pham, M.N., Sherve, M., Kumari, S., Cook, K., Pearson, J., Bogdani, M., Campbell, D.J., and Gavin, M.A. (2020). An IL-2 mutein engineered to promote expansion of regulatory T cells arrests ongoing autoimmunity in mice. Sci. Immunol. *5*, eaba5264.

24. Horwitz, D.A., Zheng, S.G., Wang, J., and Gray, J.D. (2008). Critical role of IL-2 and TGF-beta in generation, function and stabilization of Foxp3+CD4+ Treg. Eur. J. Immunol. *38*, 912–915.

25. Riolobos, L., Hirata, R.K., Turtle, C.J., Wang, P.R., Gornalusse, G.G., Zavajlevski, M., Riddell, S.R., and Russell, D.W. (2013). HLA engineering of human pluripotent stem cells. Mol. Ther. *21*, 1232–1241.

26. Wang, D., Quan, Y., Yan, Q., Morales, J.E., and Wetsel, R.A. (2015). Targeted disruption of the β2-microglobulin gene minimizes the immunogenicity of human embryonic stem cells. Stem Cells Transl. Med. *4*, 1234–1245.

27. Mattapally, S., Pawlik, K.M., Fast, V.G., Zumaquero, E., Lund, F.E., Randall, T.D., Townes, T.M., and Zhang, J. (2018). Human leukocyte antigen class I and II knockout human induced pluripotent stem cell-derived cells: universal donor for cell therapy. J. Am. Heart Assoc. *7*, e010239.

28. Gornalusse, G.G., Hirata, R.K., Funk, S.E., Riolobos, L., Lopes, V.S., Manske, G., Prunkard, D., Colunga, A.G., Hanafi, L.A., Clegg, D.O., et al. (2017). HLA-E-expressing pluripotent stem cells escape allogeneic responses and lysis by NK cells. Nat. Biotechnol. *35*, 765–772.

29. Castro-Gutierrez, R., Alkanani, A., Mathews, C.E., Michels, A., and Russ, H.A. (2021). Protecting stem cell derived pancreatic beta-like cells from diabetogenic T cell recognition. Front. Endocrinol. *12*, 707881.

30. Freeman, G.J., Long, A.J., Iwai, Y., Bourque, K., Chernova, T., Nishimura, H., Fitz, L.J., Malenkovich, N., Okazaki, T., Byrne, M.C., et al. (2000). Engagement of the PD-1 immunoinhibitory receptor by a novel B7 family member leads to negative regulation of lymphocyte activation. J. Exp. Med. *192*, 1027–1034.

31. Kleiveland, C.R. (2015). Peripheral blood mononuclear cells. In The Impact of Food Bioactives on Health: in vitro and ex vivo models, K. Verhoeckx, P. Cotter, I. López-Expósito, C. Kleiveland, T. Lea, A. Mackie, T. Requena, D. Swiatecka, and H. Wichers, eds. (Cham: Springer International Publishing).

32. Chen, L., and Flies, D.B. (2013). Molecular mechanisms of T cell co-stimulation and co-inhibition. Nat. Rev. Immunol. *13*, 227–242.

33. Garcia-Diaz, A., Shin, D.S., Moreno, B.H., Saco, J., Escuin-Ordinas, H., Rodriguez, G.A., Zaretsky, J.M., Sun, L., Hugo, W., Wang, X., et al. (2017). Interferon receptor signaling pathways regulating PD-L1 and PD-L2 expression. Cell Rep. *19*, 1189–1201.

34. Imaizumi, T., Kumagai, M., Sasaki, N., Kurotaki, H., Mori, F., Seki, M., Nishi, N., Fujimoto, K., Tanji, K., Shibata, T., et al. (2002). Interferon-gamma stimulates the expression of galectin-9 in cultured human endothelial cells. J. Leukoc. Biol. *72*, 486–491.

35. Benci, J.L., Xu, B., Qiu, Y., Wu, T.J., Dada, H., Twyman-Saint Victor, C., Cucolo, L., Lee, D.S.M., Pauken, K.E., Huang, A.C., et al. (2016). Tumor interferon signaling regulates a multigenic resistance program to immune checkpoint blockade. Cell *167*, 1540–1554.e12.

36. Wagner, A.H., Gebauer, M., Pollok-Kopp, B., and Hecker, M. (2002). Cytokine-inducible CD40 expression in human endothelial cells is mediated by interferon regulatory factor-1. Blood *99*, 520–525.

37. Rigau, M., Ostrouska, S., Fulford, T.S., Johnson, D.N., Woods, K., Ruan, Z., McWilliam, H.E.G., Hudson, C., Tutuka, C., Wheatley, A.K., et al. (2020). Butyrophilin 2A1 is essential for phosphoantigen reactivity by γδ T cells. Science *367*, eaay5516.

38. Deuse, T., Hu, X., Agbor-Enoh, S., Jang, M.K., Alawi, M., Saygi, C., Gravina, A., Tediashvili, G., Nguyen, V.Q., Liu, Y., et al. (2021). The SIRPα-CD47 immune checkpoint in NK cells. J. Exp. Med. *218*, e20200839.

39. Suzuki, D., Flahou, C., Yoshikawa, N., Stirblyte, I., Hayashi, Y., Sawaguchi, A., Akasaka, M., Nakamura, S., Higashi, N., Xu, H., et al. (2020). iPSC-derived platelets depleted of HLA class I are inert to anti-HLA class I and natural killer cell immunity. Stem Cell Rep. *14*, 49–59.

40. Augsornworawat, P., Maxwell, K.G., Velazco-Cruz, L., and Millman, J.R. (2020). Single-cell transcriptome profiling reveals β cell maturation in stem cell-derived islets after transplantation. Cell Rep. *32*, 108067.

41. Baron, M., Veres, A., Wolock, S.L., Faust, A.L., Gaujoux, R., Vetere, A., Ryu, J.H., Wagner, B.K., Shen-Orr, S.S., Klein, A.M., et al. (2016). A single-cell transcriptomic map of the human and mouse pancreas reveals inter- and intra-cell population structure. Cell Syst. *3*, 346–360.e4.

42. van der Torren, C.R., Zaldumbide, A., Duinkerken, G., Brand-Schaaf, S.H., Peakman, M., Stangé, G., Martinson, L., Kroon, E., Brandon, E.P., Pipeleers, D., and Roep, B.O. (2017). Immunogenicity of human embryonic stem cell-derived beta cells. Diabetologia *60*, 126–133.

43. Klimosch, S.N., Bartel, Y., Wiemann, S., and Steinle, A. (2013). Genetically coupled receptor–ligand pair NKp80-AICL enables autonomous control of human NK cell responses. Blood *122*, 2380–2389.

44. Brehm, M.A., Kenney, L.L., Wiles, M.V., Low, B.E., Tisch, R.M., Burzenski, L., Mueller, C., Greiner, D.L., and Shultz, L.D. (2019). Lack of acute xenogeneic graft- versus-host disease, but retention of T-cell function following engraftment of human peripheral blood mononuclear cells in NSG mice deficient in MHC class I and II expression. FASEB J. *33*, 3137–3151.

45. Viricel, C., Ahmed, M., and Barakat, K. (2015). Human PD-1 binds differently to its human ligands: a comprehensive modeling study. J. Mol. Graph. Model. *57*, 131–142.

46. Finger, L.R., Pu, J., Wasserman, R., Vibhakar, R., Louie, E., Hardy, R.R., Burrows, P.D., and Billips, L.G. (1997). The human PD-1 gene: complete cDNA, genomic organization, and developmentally regulated expression in B cell progenitors. Gene *197*, 177–187.

47. Han, X., Wang, M., Duan, S., Franco, P.J., Kenty, J.H.-R., Hedrick, P., Xia, Y., Allen, A., Ferreira, L.M.R., Strominger, J.L., et al. (2019). Generation of hypoimmunogenic human pluripotent stem cells. Proc. Natl. Acad. Sci. USA *116*, 10441–10446.

48. Leite, N.C., Pelayo, G.C., and Melton, D.A. (2022). Genetic manipulation of stress pathways can protect stem-cell-derived islets from apoptosis in vitro. Stem Cell Rep. *17*, 766–774.

49. Yang, R., Sun, L., Li, C.-F., Wang, Y.-H., Yao, J., Li, H., Yan, M., Chang, W.C., Hsu, J.M., Cha, J.H., et al. (2021). Galectin-9 interacts with PD-1 and TIM-3 to regulate T cell death and is a target for cancer immunotherapy. Nat. Commun. *12*, 832.

50. Heusschen, R., Griffioen, A.W., and Thijssen, V.L. (2013). Galectin-9 in tumor biology: a jack of multiple trades. Biochim. Biophys. Acta *1836*, 177–185.

51. Stancill, J.S., Kasmani, M.Y., Khatun, A., Cui, W., and Corbett, J.A. (2021). Single-cell RNA sequencing of mouse islets exposed to proinflammatory cytokines. Life Sci. Alliance *4*, e202000949.

52. Herndler-Brandstetter, D., Shan, L., Yao, Y., Stecher, C., Plajer, V., Lietzenmayer, M., Strowig, T., de Zoete, M.R., Palm, N.W., Chen, J., et al. (2017). Humanized mouse model supports development, function, and tissue residency of human natural killer cells. Proc. Natl. Acad. Sci. USA *114*, 9626–9634.

53. Wyburn, K.R., Jose, M.D., Wu, H., Atkins, R.C., and Chadban, S.J. (2005). The role of macrophages in allograft rejection. Transplantation *80*, 1641–1647.

54. Oberbarnscheidt, M.H., Zeng, Q., Li, Q., Dai, H., Williams, A.L., Shlomchik, W.D., Rothstein, D.M., and Lakkis, F.G. (2014). Non-self recognition by monocytes initiates allograft rejection. J. Clin. Invest. *124*, 3579–3589.

55. Zhuang, Q., Liu, Q., Divito, S.J., Zeng, Q., Yatim, K.M., Hughes, A.D., Rojas-Canales, D.M., Nakao, A., Shufesky, W.J., Williams, A.L., et al. (2016). Graft-infiltrating host dendritic cells play a key role in organ transplant rejection. Nat. Commun. *7*, 12623.

56. Muller, Y.D., Ferreira, L.M.R., Ronin, E., Ho, P., Nguyen, V., Faleo, G., Zhou, Y., Lee, K., Leung, K.K., Skartsis, N., et al. (2021). Precision engineering of an anti-HLA-A2 chimeric antigen receptor in regulatory T cells for transplant immune tolerance. Front. Immunol. *12*, 686439.

57. Hu, M., Rogers, N.M., Li, J., Zhang, G.Y., Wang, Y.M., Shaw, K., O'Connell, P.J., and Alexander, S.I. (2021). Antigen specific regulatory T cells in kidney transplantation and other tolerance settings. Front. Immunol. *12*, 717594.

58. Wagner, J.C., and Tang, Q. (2020). CAR-tregs as a strategy for inducing graft tolerance. Curr. Transplant. Rep. *7*, 205–214.

59. Lim, D., Sreekanth, V., Cox, K.J., Law, B.K., Wagner, B.K., Karp, J.M., and Choudhary, A. (2020). Engineering designer beta cells with a CRISPR-Cas9 conjugation platform. Nat. Commun. *11*, 4043.

60. Wang, X., Wang, K., Yu, M., Velluto, D., Hong, X., Wang, B., Chiu, A., Melero-Martin, J.M., Tomei, A.A., and Ma, M. (2022). Engineered immunomodulatory accessory cells improve experimental allogeneic islet transplantation without immunosuppression. Sci. Adv. *8*, eabn0071.

61. Mandal, P.K., Ferreira, L.M.R., Collins, R., Meissner, T.B., Boutwell, C.L., Friesen, M., Vrbanac, V., Garrison, B.S., Stortchevoi, A., Bryder, D., et al. (2014). Efficient ablation of genes in human hematopoietic stem and effector cells using CRISPR/Cas9. Cell Stem Cell *15*, 643–652.

62. Kaiser, B.K., Barahmand-pour, F., Paulsene, W., Medley, S., Geraghty, D.E., and Strong, R.K. (2005). Interactions between NKG2x immunoreceptors and HLA-E ligands display overlapping affinities and thermodynamics. J. Immunol. *174*, 2878–2884.

63. Wolf, F.A., Angerer, P., and Theis, F.J. (2018). SCANPY: large-scale single-cell gene expression data analysis. Genome Biol. *19*, 15.

64. Furman, B.L. (2021). Streptozotocin-induced diabetic models in mice and rats. Curr. Protoc. *1*, e78.

STAR★METHODS

KEY RESOURCES TABLE

REAGENT or RESOURCE	SOURCE	IDENTIFIER
Antibodies		
PE Mouse monoclonal anti-human HLA-ABC	Biolegend	Cat# 311405; RRID: AB_314874
PE Mouse monoclonal anti-human HLA-E	Biolegend	Cat# 342603; RRID: AB_1659250
PE Mouse monoclonal anti-human CD274 (B7-H1, PD-L1)	Biolegend	Cat# 393607; RRID: AB_2749924
Rat monoclonal anti-human C-peptide	DSHB	Cat# GN-ID4; RRID: AB_2255626
Mouse monoclonal anti-human Nkx6.1	DSHB	Cat# F55A12; RRID: AB_532379
Goat polyclonal anti-Rat IgG (H+L) Cross-Adsorbed Secondary Antibody, Alexa Fluor 647	Life Technologies	Cat# A-21247; RRID: AB_141778
Goat polyclonal anti-Mouse IgG (H+L) Cross-Adsorbed Secondary Antibody, Alexa Fluor 405	Life Technologies	Cat# A-31553; RRID: AB_221604
PE Mouse monoclonal IgG2a, κ Isotype Ctrl (FC)	Biolegend	Cat# 400213; RRID: AB_2800438
PE Mouse monoclonal IgG1, κ Isotype Ctrl	Biolegend	Cat# 400112; RRID: AB_2847829
PE Mouse monoclonal anti-human CD49a	BD Biosciences	Cat# 559596; RRID: AB_397288
Rabbit polyclonal anti-human HLA-E	Atlas Antibodies	Cat# HPA031454; RRID: AB_2673891
Goat polyclonal anti-Mouse IgG (H+L) Highly Cross-Adsorbed Secondary Antibody, Alexa Fluor 594	Life Technologies	Cat# A-11032; RRID: AB_2534091
Goat polyclonal anti-Rat IgG (H+L) Cross-Adsorbed Secondary Antibody, Alexa Fluor 488	Life Technologies	Cat# A-11006; RRID: AB_2534074
Goat polyclonal anti-Rabbit IgG (H+L) Cross-Adsorbed Secondary Antibody, Alexa Fluor 647	Life Technologies	Cat# A-21244; RRID: AB_2535812
APC Mouse monoclonal anti-human CD3	Biolegend	Cat# 300311; RRID: AB_314047
PE Rat monoclonal anti-human CD4	Biolegend	Cat# 357403; RRID: AB_2562035
Pacific Blue Mouse anti-human CD8	Biolegend	Cat# 344717; RRID: AB_10551616
Pacific Blue Mouse monoclonal anti-human CD56 (NCAM)	Biolegend	Cat# 362519; RRID: AB_2564096
Pacific Blue Mouse monoclonal IgG1, κ Isotype Ctrl	Biolegend	Cat# 400131; RRID: AB_2923473
APC Mouse monoclonal IgG2a, κ Isotype Ctrl	Biolegend	Cat# 400221; RRID: AB_2891178
PE Rat monoclonal IgG2b, κ Isotype Ctrl	Biolegend	Cat# 400607; RRID: AB_326551
Ultra-LEAF Purified Mouse monoclonal anti-human TIGIT (VSTM3)	Biolegend	Cat# 372719; RRID: AB_2650966
Pacific Blue Mouse monoclonal anti-human CD31	Biolegend	Cat# 303113; RRID: AB_1877196
APC Mouse monoclonal anti-human CD47	Biolegend	Cat# 323123; RRID: AB_2716202
APC Mouse monoclonal anti-human CD324 (E-Cadherin)	Biolegend	Cat# 324107; RRID: AB_756069
PE Mouse monoclonal anti-human CD325 (N-Cadherin)	Biolegend	Cat# 350806; RRID: AB_10660824
PE Mouse monoclonal anti-human CD112 (Nectin-2)	Biolegend	Cat# 337409; RRID: AB_2174163
APC Mouse monoclonal anti-human CD155 (PVR)	Biolegend	Cat# 337617; RRID: AB_2565814
PE Mouse monoclonal anti-human CD111 (Nectin-1)	Biolegend	Cat# 340404; RRID: AB_2174152
APC Mouse monoclonal anti-human MICA/MICB	Biolegend	Cat# 320907; RRID: AB_493196
Alexa Fluor 647 Mouse monoclonal anti-human/mouse/rat PCNA	Biolegend	Cat# 307912; RRID: AB_2267947
PE Rabbit monoclonal anti-human BAT3/BAG-6	Abcam	Cat# ab210838; RRID: AB_2923475
APC Mouse monoclonal anti-human CD48	Biolegend	Cat# 336713; RRID: AB_2810516
PE Mouse monoclonal anti-human CD70	Biolegend	Cat# 355103; RRID: AB_2561430
Mouse monoclonal anti-human Nectin-3/PVRL3 (CD113)	Millipore-Sigma	Cat# MABT63; RRID: AB_10807983
APC Mouse monoclonal anti-human ULBP1	R&D Systems	Cat# FAB1380A; RRID: AB_2923476
PE Mouse monoclonal anti-human ULBP2/5/6	R&D Systems	Cat# FAB1298P; RRID: AB_2214693
APC Mouse monoclonal anti-human OCIL/CLEC2D	R&D Systems	Cat# FAB3480A; RRID: AB_2044641
PE Mouse monoclonal anti-human CD72	Biolegend	Cat# 316207; RRID: AB_2819945

(*Continued on next page*)

Continued

REAGENT or RESOURCE	SOURCE	IDENTIFIER
APC Mouse monoclonal IgG1, κ Isotype Ctrl	Biolegend	Cat# 400121; RRID: AB_326443
APC Mouse monoclonal IgG2a, κ Isotype Ctrl	Biolegend	Cat# 400221; RRID: AB_2891178
PE Mouse monoclonal IgG2a, κ Isotype Ctrl	Biolegend	Cat# 400213; RRID: AB_2800438
APC Rat monoclonal IgG1, λ Isotype Ctrl	Biolegend	Cat# 401903; RRID: AB_292347
PE Rabbit (DA1E) mAb IgG XP Isotype Control	Cell Signalling Technology	Cat# 5742; RRID: AB_10694219
Goat ploYclonal anti-Mouse IgG (H+L) Cross-Adsorbed Secondary Antibody, Alexa Fluor 488	Life Technologies	Cat# A-11001; RRID: AB_2534069
PE Mouse monoclonal anti-human CD159c (NKG2C)	Biolegend	Cat# 375003; RRID: AB_2888871
APC Mouse monoclonal anti-human CD159a (NKG2A)	Biolegend	Cat# 375107; RRID: AB_2888862
APC Mouse monoclonal anti-human TIGIT (VSTM3)	Biolegend	Cat# 372705; RRID: AB_2632731
PE Mouse monoclonal anti-human KLRG1	Biolegend	Cat# 368609; RRID: AB_2572136
APC Mouse monoclonal anti-human CD96 (TACTILE)	Biolegend	Cat# 338409; RRID: AB_2566141
PE Mouse monoclonal anti-human CD172a (SIRPα)	Biolegend	Cat# 372103; RRID: AB_2650860
PE/Cyanine7 Mouse monoclonal anti-human CD337 (NKp30)	Biolegend	Cat# 325213; RRID: AB_2716064
APC Mouse monoclonal anti-human CD335 (NKp46)	Biolegend	Cat# 331917; RRID: AB_2561649
PE Mouse monoclonal anti-human NKp80	Biolegend	Cat# 346706; RRID: AB_1967147
APC Mouse monoclonal anti-human CD226 (DNAM-1)	Biolegend	Cat# 338311; RRID: AB_2561951
PE Mouse monoclonal anti-human CD314 (NKG2D)	Biolegend	Cat# 320805; RRID: AB_492961
APC Mouse monoclonal IgG2a, κ Isotype Ctrl	Biolegend	Cat# 400221; RRID: AB_2891178
PE/Cyanine7 Mouse monoclonal IgG1, κ Isotype Ctrl	Biolegend	Cat# 400125; RRID: AB_2861433
Guinea Pig polyclonal anti-human Insulin	DAKO	Cat# A0564; RRID: AB_10013624
Rat monoclonal anti-mouse CD8a	Biolegend	Cat# 100702; RRID: AB_312741
Mouse monoclonal anti-mouse FOXP3	Biolegend	Cat# 320002; RRID: AB_439746
Goat polyclonal anti-Guinea Pig IgG (H+L) Highly Cross-Adsorbed Secondary Antibody, Alexa Fluor 647	Life Technologies	Cat# A-21450; RRID: AB_2735091
Bacterial and virus strains		
One Shot™ Stbl3™ Chemically Competent *E. coli*	Thermofisher	Cat# C737303
Biological samples		
Aphaersis leukoreduction collars	BWH, Boston	N/A
Human islets	Prodo Laboratories	N/A
Chemicals, peptides, and recombinant proteins		
mTesR1	Stemcell Technologies	Cat# 85850
Alt-R® S.p. HiFi Cas9 Nuclease V3	IDT	Cat# 1081059
Y27632	DNSK	Cat# DNSK-KI-15-02
Corning® Matrigel® hESC-Qualified Matrix, LDEV-free	Corning	Cat# 354277
rhIFN-γ	R&D Systems	Cat# 285-IF-100
CloneR	Stemcell Technologies	Cat# 05888
Accutase	Stemcell Technologies	Cat# 07920
Phosphate Buffered Saline	Corning	Cat# 21040CV
Bovine Serum Albumin	Gibco	Cat# A10008-01
Donkey Serum	Jackson Labs	Cat# 100181-234
Paraformaldehyde	EMS	Cat# 15710
OCT compound	Tissue Tek	Cat# 4583
Histo-Clear	EMS	Cat# 64110-01
Triton X-100	Millipore-Sigma	Cat# 9036-19-5
Vectashied with DAPI	Vector Laboratories	Cat# H-1200
Lymphoprep	Stemcell Technologies	Cat# 07801
CryoStor CS10	Stemcell Technologies	Cat# 07930

(*Continued on next page*)

Continued

REAGENT or RESOURCE	SOURCE	IDENTIFIER
D-luciferin, Potassium Salt	Gold Biotechnology	Cat# 115144-35-9
ImmunoCult™-XF T Cell Expansion Medium	Stemcell Technologies	Cat# 10981
rhIL-2	Peprotech	Cat# 200-02
NK MACS medium	Milteny Biotec	Cat# 130-114-429
Human AB serum	Valley Biomed	Cat# HP1022HI
HyClone FBS	GE Healthcare	Cat# SH30070.03
Matrigel® Basement Membrane Matrix, Phenol Red-free, LDEV-free	Corning	Cat# 356237
Streptozotocin	Millipore-Sigma	Cat# S0130-50MG
TrypLE Express	Thermofisher	Cat# 12604013
Vectashield with DAPI	Vector Laboratories	Cat# H-1200
Critical commercial assays		
RosetteSep Human CD4$^+$ T Cell Enrichment Cocktail	Stemcell Technologies	Cat# 15062
RosetteSep CD8$^+$ T Cell Enrichment Cocktail	Stemcell Technologies	Cat# 15063
RosetteSep NK Cell Enrichment Cocktail	Stemcell Technologies	Cat# 15065
STEMdiff™ Endothelial Differentiation Kit	Stemcell Technologies	Cat# 08005
ImmunoCult™ Human CD3/CD28 T Cell Activator	Stemcell Technologies	Cat# 10991
RNeasy Plus Mini Kit	Qiagen	Cat# 74134
SMART-Seq v4 Ultra Low Input Kit for Sequencing	Clontech	Cat# 634894
Illumina Nextera XT library	Illumina	Cat# FC-131-1096
Human Ultrasensitive Insulin ELISA	ALPCO Diagnostics	Cat# 80-INSHUU-E01.1.
Legend Max IL-2 ELISA	Biolegend	Cat# 431807
Legend Max TGF-β ELISA	Biolegend	Cat# 436707
Legend Max IL-10 ELISA	Biolegend	Cat# 430607
Deposited data		
Bulk RNA sequencing	https://www.ncbi.nlm.nih.gov/geo/	Accession no. GSE200021
Experimental models: Cell lines		
NK-92mi	ATCC	Cat# CRL-2408
K562-Luc2	Biocytogen	Cat# BCG-PS-015-luc
Raji-GFP-Luc2	Biocytogen	Cat# BCG-PS-087-luc
HUES 8 hESC line (NIH approval number NIHhESC-09-0021)	HSCI iPS Core	hES Cell Line: HUES-8
Experimental models: Organisms/strains		
B6(Cg)-Tyrc-2J/J mice	Jackson Labs	Cat# 000058
CB17.Cg-PrkdcscidLystbg-J/Crl mice	Charles River Labs	Cat# 250
NSG-(K^bD^b)^{null} (IA)^{null} mice	Jackson Labs	Cat# 025216
NOD/ShiLtJ mice	Jackson Labs	Cat# 001976
Recombinant DNA		
B2M gRNA 5′-GCTACTCTCTCTTTCTGGCC′3	IDT	N/A
PD-L1 gBlock	Genscript, this paper	N/A
peptide::B2M::HLA-E fusion gBlock	Genscript, this paper	N/A
IL-2 mutein-TGFβ-IL-10 gBlock	Genscript, this paper	N/A
Software and algorithms		
FlowJo 10.7.1	BD Biosciences	https://www.flowjo.com/solutions/flowjo/downloads
Living Image	PerkinElmer	Cat# 128113
MARS data analysis	BMG LABTECH	https://www.bmglabtech.com/en/microplate-reader-software/
BD FACSDiva v9.0	BD Biosciences	N/A

(*Continued on next page*)

Continued

REAGENT or RESOURCE	SOURCE	IDENTIFIER
HiSeq Control Software	Illumina	N/A
bcl2fastq 2.17 Software	Illumina	N/A
Trimmomatic v.0.36	USADELLAB	http://www.usadellab.org/cms/?page=trimmomatic
STAR aligner v.2.5.2b	N/A	https://github.com/alexdobin/STAR
DESeq2	N/A	https://bioconductor.org/packages/release/bioc/html/DESeq2.html
Prism v9	Graphpad	https://www.graphpad.com/scientific-software/prism/
Other		
4D Nucleofector	Lonza	Cat# AAF-1003B
FACS Aria II flow cytometer	BD Biosciences	N/A
LSR II flow cytometer	BD Biosciences	N/A
Zeiss Axio Imager Z2 with Apotome microscope	Zeiss	N/A
IVIS SpectrumCT	PerkinElmer	128201
CLARIOstar Plus microplate reader	BMG LABTECH	https://www.bmglabtech.com/en/clariostar-plus/
Illumina HiSeq 2000	Illumina	Cat# SY-401-1001
Vi-CELL XR Cell Viability Analyser	Beckman Coulter	Cat# 731050
Qubit Fluorometer	Thermofisher	N/A

RESOURCE AVAILABILITY

Lead contact

Further information and requests for resources and reagents should be directed to and will be fulfilled by the lead contact, Douglas A. Melton (dmelton@harvard.edu).

Materials availability

Gene-modified HUES8 lines used in this study are available upon request; additionally, the reagents used in this study are available from the lead contact with a completed Materials Transfer Agreement.

Data and code availability

Bulk SC-β and SC-Endothelial cell RNA sequencing data has been submitted to the NIH Gene Expression Omnibus (GEO) repository and is available under accession GSE200021. This manuscript analyzes existing, publicly available data. The accession numbers for the datasets are listed in the key resources table. This paper does not report original code. Any additional information required to reanalyze the data reported in the work paper is available from the lead contact upon request.

EXPERIMENTAL MODEL AND SUBJECT DETAILS

Mice

Male (6–8 weeks of age) B6(Cg)-Tyrc-2J/J (B6/abino; Jackson Labs, #000058), CB17.Cg-PrkdcscidLystbg-J/Crl (Scid/beige; Charles River Labs, #250), NSG-(K^bD^b)^{null} (IA)^{null} (NSG-MHC Class I/II KO; Jackson Labs, #025216) and female (10 weeks of age) NOD/ShiLtJ (NOD; Jackson Labs, #001976) were purchased. Mice were housed in specific pathogen-free conditions at Harvard University. All animal research was conducted under Harvard IACUC approval.

Cell lines

Human ES maintenance and differentiation was carried out as previously described.[3,5] SC-islet cell differentiations were initiated 72 h after initial passage by aspirating mTeSR1 (STEMCELL Technologies, 85850) and replenished with stage and day-specific media supplemented with the appropriate small molecules or growth factors as previously described.[7] All cell lines (GAPluc, B2M$^{-/-}$, GAP-PD, GAP-B2P, GAP-BEC and 2B10) were routinely tested for mycoplasma and were mycoplasma-free. All experiments involving human ES cells were approved by the Harvard University ESCRO (#E00024) committee.

Human samples

The study was carried out in accordance with the Harvard University guidelines and was approved by the University of Massachusetts (UMASS) institutional review board ethics (IRB14-4650) committee. Informed consent was obtained from the patients and healthy donors before blood donation. All blood samples were received as de-identified, therefore, the information on the age and/or gender of the donors is not available.

Primary immune cells

PBMCs, CD8 and CD4 T cells were isolated and maintained in ImmunoCult™-XF T Cell Expansion Medium (STEMCELL Technologies, 10981) + 100U/mL rhIL-2 (Peprotech, 200-02). NK cells were isolated and maintained in NK cell medium (NK MACS medium (Milteny Biotec, 130-114-429) + 5% Human AB serum (Valley Biomed, HP1022HI) + 5% HyClone FBS (GE Healthcare) + 0.5 ng/mL rhIL-2). Details of specific culture conditions can be found in the STAR Methods details.

METHOD DETAILS

Generation of hypo-immunogenic hESCs

The existing GAPluc (WT) hESC line served as starting material for the generation of HLA-deficient hESCs.[20] To generate HLA-deficient hESCs, 1 × 10^6 WT hESCs were nucleofected using the 4D-Nucleofector (Lonza) with RNP complexed with 120 pmol B2M gRNA (5′-GCTACTCTCTCTTTCTGGCC′3)[61] (IDT) and 104 pmol Alt-R® S.p. HiFi Cas9 Nuclease V3 (IDT) according to the manufacturer's instructions. Nucleofected cells were resuspended in mTesR1 + 10 μM Y27632 (DNSK International, DNSK-KI-15-02) and plated in a matrigel-coated tissue culture plate. After 48 h cells were treated with 10 ng/mL IFN-γ (R&D, 285-IF-100) for 24 h and then stained with APC anti-human HLA-ABC (W6/32, 1:100) (Biolegend, 311409). HLA-$ABC^{-/-}$ cells were sorted on a FACS Aria II (BD Biosciences) and plated in a matrigel-coated tissue culture plate containing mTesR1 + CloneR (STEMCELL Technologies, 05888), with single colonies picked for expansion. The resulting HLA-deficient line was named $B2M^{-/-}$.

To generate GAP-PD and GAP-BEC hESCs, human PD-L1 and the peptide::B2M::HLA-E fusion sequences were synthesized as gBlocks (Genscript) and cloned into our existing GAPluc targeting plasmid downstream of the *Luc2* gene. The sequence of the covalently attached peptide (VMAPRTLLL) in the peptide::B2M::HLA-E fusion is derived from the HLA-Cw7 molecule.[62] hESCs were nucleofected with the GAP-PD or GAP-BEC targeting plasmids and GAPDH-targeting RNP as previously described.[20] For GAP-B2P and GAP-BEC lines, a polyclonal population of puromycin-selected cells was subsequently nucleofected with B2M-targeting RNP, and single-colonies were picked for expansion after FACS sorting as described above. The gating strategy for sorting HLA-$ABC^{-/-}$ hESCs is described in Figure S1I.

Flow cytometry

Differentiated WT, $B2M^{-/-}$, BEC, PD-L1 and B2P SC-islet cells were both treated and untreated with 10 ng/mL IFN-γ for 24 h prior to staining. Cells were dissociated with Accutase (STEMCELL Technologies, 07920), washed twice with PBS + 0.1% BSA (Gibco, A10008-01) and blocked for 30 min on ice with PBS + 5% donkey serum (Jackson Labs; 100181-234). Cells were then stained for 30 min on ice in blocking buffer with PE or APC anti-human HLA-ABC (Biolegend, 311405), PE anti-human HLA-E (Biolegend, 342603) and PE anti-human PD-L1 (Biolegend, 393607). Cells were then washed three times and fixed in 4% PFA (EMS, 15710) for 15 min at 4°C. Fixed cells were then incubated in blocking buffer with rat anti-human C-peptide (DHSB; GN-ID4) and mouse anti-human Nkx6.1 (DHSB; F55A12) (overnight at 4°C), washed three times with blocking buffer, incubated with goat anti-rat 647 (Life Technologies, A-21247; 1:300) and goat anti-mouse 405 (Life Technologies, A-31553; 1:300) in blocking solution (1 h at room temperature), washed three times and resuspended in PBS +0.1% BSA. Samples were captured on the LSR II (BD) flow cytometer and analyzed using BD FACSDiva v9.0 (BD Biosciences) and FlowJo 10.7.1 (BD). All antibodies were used at 1:100 unless otherwise stated. The gating strategy for identifying SC-β cells is described in Figure S1J. PE mouse IgG2a (Biolegend, 400213) and PE mouse IgG1 (Biolegend, 400111) served as isotype controls.

Magnetic enrichment using CD49a and reaggregation

WT and BEC SC-β cells were magnetically enriched from SC-islet clusters as previously described.[7] Enriched cells were resuspended in S6 medium and plated at 5 × 10^3 cells/well in low-attachment 96-well v-bottom tissue-culture plates (Thermo Scientific, 277143), centrifuged at 300 g for 1 min and incubated at 37°C for 4–7 days. CD49a enriched SC-β cell clusters were fed fresh S6 medium every 2 days.

SC-β cell immunohistochemistry

$CD49a^+$ enriched SC-β cell clusters were fixed in 4% PFA for 1 h at room temperature, washed and frozen in OCT (Tissue-Tek, 4583) and sectioned to 14 μm. For staining, slides were incubated in blocking buffer (PBS + 0.1% Triton-X + 5% donkey serum) for 1 h at room temperature, incubated in PBS + 5% donkey serum containing rat anti-human C-peptide (1:300), mouse anti-human Nkx6.1 (1:100) and rabbit anti-human HLA-E (Atlas Antibodies, HPA031454, 1:100) for 1 h at room temperature, washed three times, incubated in goat anti-mouse 594 (Life Technologies, A-11032; 1:500), goat anti-rat 488 (Life Technologies, A-11006; 1:500) and goat anti-rabbit 647 (Life technologies, A-21244; 1:500) for 2 h at room temperature, washed, mounted in Vectashield with DAPI (Vector

Laboratories; H-1200), covered with coverslips and sealed with clear nail polish. Representative regions were imaged using Zeiss.Z2 with Apotome microscope (Zeiss) and analyzed using Zen Blue v2 (Zeiss).

Immune cell isolation and identification

PBMCs, CD8 and CD4 T cells, and NK cells were isolated from apheresis leukoreduction collars ($n = 5$ donors) obtained from Brigham and Women's Hospital in compliance with our IRB approval. PBMCs were isolated by density gradient centrifugation with lymphoprep (STEMCELL Technologies, 07801) SepMate^{TM}-50 (IVD) tubes (STEMCELL Technologies, 85450) according to the manufacturer's instructions. CD4, CD8 and NK cells were isolated by density gradient centrifugation with lymphoprep and SepMate^{TM}-50 (IVD) tubes following the addition of RosetteSep Human CD4^{+} T Cell Enrichment Cocktail (STEMCELL Technologies, 15062), CD8^{+} T Cell Enrichment Cocktail (STEMCELL Technologies, 15063) and NK Cell Enrichment Cocktail (STEMCELL Technologies, 15065) respectively. Enriched immune cells were cryopreserved in CryoStor CS10 (STEMCELL Technologies, 07930) at a concentration of 10M cells/vial.

Flow cytometric analysis of enriched immune cell subpopulations was performed by staining cells in blocking buffer containing APC anti-human CD3 (Biolegend, 300311), PE anti-human CD4 (Biolegend, 357403), Pacific Blue anti-human CD8 (Biolegend, 344717) and Pacific Blue anti-human CD56 (Biolegend, 362519). Isotype controls were Pacific Blue mouse IgG1 (Biolegend, 400131), APC mouse IgG2a (Biolegend, 400221) and PE rat IgG2b (Biolegend, 400607). All antibodies were used at 1:100 or unless otherwise stated. Representative gating strategies are demonstrated in Figures S2G–S2I.

Xenotransplantation of SC-islets in B6/albino mice

WT, PD-L1 and B2P SC-islet cell clusters (5×10^6 cells) were transplanted under the kidney capsule of B6/albino mice ($n = 5$/group) and graft survival was monitored for 10 days following i.p. injection of D-luciferin (Gold Biotechnology, 115144-35-9) by bioluminescence imaging on the IVIS SpectrumCT (PerkinElmer, 128201) and analyzed using Living Image Software (PerkinElmer, 128113).

In vitro T cell cytotoxicity assays

WT, B2M$^{-/-}$ and BEC SC-islet cells were seeded in S3 medium at 5×10^4 cells/well of a matrigel-coated 96-well black flat-bottom plate (Corning, 3916) in the presence or absence of IFN-γ (10 ng/mL). After 24 h, the medium was switched to T cell medium (ImmunoCult^{TM}-XF T Cell Expansion Medium (STEMCELL Technologies, 10981) + 100U/mL rhIL-2 (Peprotech, 200-02)) for immune cell co-culture. Primary human PBMCs, CD4 or CD8 cells ($n = 5$ donors) cultured in T cell medium were added to SC-islet cells at 1:1 and 3:1 effector:target ratios with and without the addition of ImmunoCult^{TM} Human CD3/CD28 T Cell Activator (STEMCELL Technologies, 10991). All T cell cytotoxicity assays were co-cultured for 72 h, after which luminescence was measured following the addition of 150 μg/mL D-luciferin on the CLARIOstar Plus microplate reader (BMG LABTECH) and analyzed using MARS data analysis (BMG LABTECH). SC-islet cell survival was calculated as a percentage relative to luminescence in the absence of T cells (test SC-islet cell luminescence/no T cell SC-islet cell luminescence x 100).

In vitro NK cell cytotoxicity assays

WT, B2M$^{-/-}$ and BEC SC-islet cells were seeded in NK cell medium (NK MACS medium (Milteny Biotec, 130-114-429) + 5% Human AB serum (Valley Biomed, HP1022HI) + 5% HyClone FBS (GE Healthcare) + 0.5 ng/mL rhIL-2) at 2×10^4 cells/well of a 96-well black round-bottom ultra-low attachment plate (Corning, 4591). Primary NK cells ($n = 5$ donors) or NK-92 MI cells (ATCC, CRL-2408) cultured in NK cell media for 5 days were added to SC-islet cells at 1:1 and 10:1 effector:target ratios. K562-Luc2 (Biocytogen, BCG-PS-015-luc) and Raji-GFP-Luc2 (Biocytogen, BCG-PS-087-luc) cells were used as positive and negative controls respectively. In some experiments, primary NK cells were pre-treated with 50 ug/mL anti-human TIGIT (Biolegend, 372719) or anti-SIRPα blocking peptide (MyBiosource, MBS822365) for 2 h and during the assay. All NK cell cytotoxicity assays were co-cultured for 5 h, after which luminescence and SC-islet cell survival was measured as described above.

In vivo NK cell cytotoxicity

2.5×10^5 WT and B2M$^{-/-}$ SC-islet cell clusters were resuspended either alone or with 7.5×10^5 primary human NK cells (pre-treated with 0.5 ng/mL rhIL-2 for 12 h) in phenol-free Matrigel (Corning, 356237) and transplanted subcutaneously in Scid/beige mice ($n = 5$). Bioluminescence was measured 10 min after i.p injection of 10 μL/g D-luciferin (15 mg/mL) on days 1 and 5 following cell transplantation on the IVIS SpectrumCT as previously described.[20]

Single cell RNA-sequencing analyses

For RNA expression analysis, datasets from[41] and[7] were downloaded from GSE114412, and for[40] from GSE151117. Data was re-analyzed using Scanpy.[63] For Baron et al.[41] and Veres et al.,[7] pseudobulk TPM values were used as previously published. For Augsornworawat et al.,[40] pseudobulk values were computed using the original cell type labels provided by the authors, by summing raw counts across labeled cells, followed by TPM normalization.

Endothelial cell differentiation

WT and B2M$^{-/-}$ hESCs were seeded in mTesR1 + 10 μM Y27632 at a concentration of 7.5×10^4 cells/well of a Matrigel-coated 6-well tissue-culture plate (Corning, 3516). Thereafter, cells were differentiated into endothelial cells using STEMdiff^{TM} Endothelial

Differentiation Kit (STEMCELL Technologies, 08005) according to the manufacturer's instructions. Differentiation efficiency was quantified by FACS analysis after staining endothelial cells with Pacific Blue anti-human CD31 (Biolegend, 303113). Pacific Blue mouse IgG1 (Biolegend, 400131) was used as an isotype control. All antibodies were used at 1:100 unless otherwise stated.

Bulk RNA sequencing

Magnetically-enriched CD49a$^+$ SC-β cells and SC-Endothelial cells were seeded in 6-well plates at 1 × 10^6 cells/well (in triplicate) and treated with and without 10 ng/mL IFN-γ for 24 h. Cells were then harvested using Accutase and the pellets snap-frozen on dry-ice. RNA extractions, library preparations and sequencing reactions were conducted at GENEWIZ, LLC. (South Plainfield, NJ, USA). Total RNA was extracted from cell pellet samples using RNeasy Plus Mini Kit (Qiagen, Germantown, MD, USA) and quantified using Qubit Fluorometer (Life Technologies, Carlsbad, CA, USA). SMART-Seq v4 Ultra Low Input Kit for Sequencing was used for full-length cDNA synthesis and amplification (Clontech, 634894), and Illumina Nextera XT library (Illumina, FC-131-1096) was used for sequencing library preparation.

Multiplexed sequencing libraries were loaded on the Illumina HiSeq 2000 instrument (Illumina, SY-401-1001) and sequenced using a 2 × 150 Paired End (PE) configuration. Image analysis and base calling were conducted by the HiSeq Control Software (HCS). Raw sequence data (.bcl files) generated from Illumina HiSeq was converted into FASTQ files and de-multiplexed using Illumina's bcl2fastq 2.17 software. One mismatch was allowed for index sequence identification.

After investigating the quality of the raw data, sequence reads were trimmed to remove possible adapter sequences and nucleotides with poor quality using Trimmomatic v.0.36. The trimmed reads were mapped to the *Homo sapiens* reference genome available on ENSEMBL using the STAR aligner v.2.5.2b. The STAR aligner is a splice aligner that detects splice junctions and incorporates them to help align the entire read sequences. BAM files were generated as a result of this step. Unique gene hit counts were calculated by using feature Counts from the Subread package v.1.5.2. Only unique reads that fell within exon regions were counted.

After extraction of gene hit counts, the gene hit counts table was used for downstream differential expression analysis. Using DESeq2, a comparison of gene expression between the groups of samples was performed. The Wald test was used to generate p values and Log2 fold changes. Genes with adjusted p values <0.05 and absolute log2 fold changes >1 were called differentially expressed genes for each comparison.

NK cell ligand analysis

WT and B2M−/− SC-islet cells and SC-endothelial cells were washed twice with washing buffer and blocked for 30 min on ice with blocking buffer. Cells were then stained for 30 min on ice in blocking buffer with APC anti-human CD47 (Biolegend, 323123), APC anti-human CD324 (E-Cadherin) (Biolegend, 324107), PE anti-human CD325 (N-Cadherin) (Biolegend, 350806), PE anti-human CD112 (Nectin-2) (Biolegend, 337409), APC anti-human CD155 (PVR) (Biolegend, 337617), PE anti-human CD111 (Nectin-1) (Biolegend, 340404), APC anti-human MICA/MICB (Biolegend, 320907), AF647 anti-human PCNA (Biolegend, 307912), PE anti-human BAG6 (Abcam, ab210838), APC anti-human CD48 (Biolegend, 336713), PE anti-human CD70 (Biolegend, 355103), mouse anti-human CD113 (Nectin-3) (Millipore-Sigma, MABT63), APC anti-human ULBP1 (R&D, FAB1380A), PE anti-human ULBP2/5/6 (R&D, FAB1298P), APC anti-human CLEC2D (R&D, FAB3480A) and PE anti-human CD72 (Biolegend, 316207). PE Mouse IgG1 (Biolegend, 400112), APC mouse IgG1 (Biolegend, 400121), APC mouse IgG2a (Biolegend, 400221), PE Mouse IgG2a (Biolegend, 400213), APC rat IgG1 (Biolegend, 401903), PE rabbit IgG (Cell Signaling technology, 5742S) and goat anti-mouse 488 (Thermofisher, A-11001, 1:300) served as isotype controls. All antibodies were used at 1:100 unless otherwise stated.

NK cell receptor analysis

Primary NK or NK92mi cells were washed twice with washing buffer and blocked for 30 min on ice with blocking buffer. Cells were then stained for 30 min on ice in blocking buffer with Pacific Blue anti-human CD56 (Biolegend, 362519, 1:100), PE anti-human NKG2C (Biolegend, 375003, 1:100) and APC anti-human NKG2A (Biolegend, 375107, 1:100), APC anti-human TIGIT (Biolegend, 372705), PE anti-human KLRG1 (Biolegend, 368609), APC anti-CD96 (Biolegend, 338409), PE anti-human SIRPα (Biolegend, 372103), PE/Cy7 anti-human NKp30 (Biolegend, 325213), APC anti-human NKp46 (Biolegend, 331917), PE anti-human NKp80 (Biolegend, 346706), APC anti-human DNAM-1 (Biolegend, 338311) and PE anti-human NKG2D (Biolegend, 320805). Cells were then washed three times and resuspended in PBS + 0.1% BSA for analysis. Pacific Blue mouse IgG1 (Biolegend, 400131), PE mouse IgG1 (Biolegend, 400111), APC mouse IgG1 (Biolegend, 400121), APC mouse IgG2a (Biolegend, 400221), PE mouse IgG2a (Biolegend, 400213) and PE/Cy7 mouse IgG1 (Biolegend, 400125) served as isotype controls. All antibodies were used at 1:20 unless otherwise stated.

Transplantation of HLA-deficient SC-islet cells in humanized mice

Diabetes was induced in NSG-MHC Class I/II KO mice by multiple low-dose (40 mg/kg) streptozotocin (STZ) (Millipore-Sigma, S0130-50MG) i.p. injection as previously described.[64] Once animals reached a blood glucose of >500 mg/dL, 5 × 10^6 WT or B2M$^{-/-}$ SC-islet cells were transplanted under the kidney capsule (n = 12) as previously described.[3,5] Blood glucose and body weight was measured twice a week after transplantation.

Ten weeks after transplantation (before PBMC injection) and seven weeks after PBMC injection the function of transplanted cells was assessed by performing *in vivo* peritoneal glucose-stimulated insulin secretion (IPGTT) as previously described.[3,5] Insulin secretion was quantified using the Human Ultrasensitive Insulin ELISA (ALPCO Diagnostics; 80-INSHUU-E01.1.)

Generation of immune-tolerizing SC-islet cells

The cDNAs of human IL-2 mutein, TGF-β and IL-10 were synthesized as a polycistronic gBlock (Genscript) and cloned into the existing GAPluc targeting plasmid as described above to generate the 2B10 plasmid. The human IL-2 sequence was modified by substituting a single amino acid (N88D) as previously described.[22] 2B10 hESCs were generated by co-nucleofection of the 2B10 targeting plasmid and the GAPDH-targeting RNP as described above. 2B10 SC-islet cells were differentiated as previously described.[3,5]

In vitro glucose-stimulated insulin secretion

In vitro function was assessed by measuring glucose-stimulated insulin secretion (GSIS) as previously described.[3,5] SC-islet clusters and primary human islets (Prodo Laboratories) were washed twice in Krebs buffer (KRB), and preincubated at 37°C for 1 h in KRB containing 2.8 mM glucose (low glucose). Clusters were then challenged with three sequential treatments of alternating low-high-low KRB containing glucose (high; 20 mM), followed by depolarization with low KRB containing 30 mM KCl. Each treatment lasted 30 min, after which 100 μL of supernatant was collected and human insulin quantified using the Human Ultrasensitive Insulin ELISA. Human insulin measurements were normalized by viable cell counts that were acquired by dispersing clusters with TrypLE Express (Thermofisher, 12604013) and counted using a ViCell (Beckman Coulter).

In vitro SC-islet cell cytokine secretion and PBMC cytotoxicity assays

2B10 SC-islet cell clusters were dispersed with TrypLE Express and seeded in 96-well matrigel-coated plates in S3 media at a linear concentration (1, 2, 4, 6, 8 × 10^4, and 1 × 10^5 cells/well) in duplicate. After 24 h, supernatants were collected, centrifuged at 3000g for 5 min and the cytokines IL-2, TGF-β and IL-10 quantified using Legend Max ELISAs (IL-2, Biolegend, 431807; TGF-β, Biolegend, 436707; IL-10, Biolegend, 430607) according to the manufacturer's instructions. For cytotoxicity assays, WT and 2B10 SC-islet cells were co-cultured with human PBMCs as described above.

Xenotransplantation of 2B10 SC-islet cells in B6/albino mice

WT and 2B10 SC-islet cell clusters (5 × 10^6 cells) were transplanted under the kidney capsule of B6/albino mice (n = 4/group; of which one animal per group was sacrificed at 5 weeks post-transplantation for immunohistochemistry) and graft survival was monitored weekly for nine weeks by bioluminescence imaging following i.p. injection of D-luciferin as described above. At five weeks post-transplantation SC-islet grafts were removed for immunohistochemical analysis of surviving INS^+ cells and $CD8^+$ T and $FOXP3^+$ T_{reg} cells.

Immunohistochemistry of SC-islet grafts

The kidneys of B6/Albino mice transplanted with WT and 2B10 SC-islets were excised, fixed overnight in 4% paraformaldehyde (PFA) at room temperature and embedded in paraffin. Sections were pre-cleared with Histo-Clear, rehydrated using an ethanol gradient and antigen fixed by incubating in boiling antigen retrieval reagent (10 mM sodium citrate, pH 6.0) for 50 min. Slides were then blocked in 5% donkey serum for 1h and stained with Guinea pig anti-human Insulin (DAKO, A0564), Rat anti-mouse CD8α (Biolegend, 100702) and Mouse anti-mouse FOXP3 (Biolegend, 320002) overnight at 4°C. The slides were then washed three times, incubated in secondary antibodies goat anti-mouse 594 (Life Technologies, A-11032), goat anti-rat 488 (Life Technologies, A-11006) and goat anti-guinea pig 647 (Life technologies, A-21450) for 2 h at room temperature, washed, mounted in Vectashield with DAPI (Vector Laboratories; H-1200), covered with coverslips and sealed with clear nail polish. Representative regions were imaged using Zeiss.Z2 with Apotome microscope. All primary and secondary antibodies were used at dilution of 1:200 and 1:500 respectively.

Correction of autoimmune diabetes by 2B10 SC-β cells in NOD mice

Once female NOD mice had blood glucose concentrations >250 mg/dL (~12 weeks of age), $CD49a^+$ magnetically enriched and re-aggregated WT and 2B10 SC-β cell clusters (2 × 10^6 cells) were transplanted under the kidney capsule. Graft survival was monitored by measuring blood glucose levels weekly for 8 weeks.

QUANTIFICATION AND STATISTICAL ANALYSIS

All data are presented as means ± SD and were analyzed by GraphPad Prism 9 (GraphPad Software). Statistically significant differences were determined either by one-way or two-way ANOVA, with Tukey's and Sidak's post-hoc test for multiple comparisons, and two-tailed t test for pairwise comparisons. p values are indicated in the figures as *$p < 0.05$, **$p < 0.01$, ***$p < 0.005$ and ****$p < 0.001$.

Cell Reports Medicine, Volume *4*

Supplemental information

Engineering human stem cell-derived islets to evade immune rejection and promote localized immune tolerance

Dario Gerace, Quan Zhou, Jennifer Hyoje-Ryu Kenty, Adrian Veres, Elad Sintov, Xi Wang, Kyle R. Boulanger, Hongfei Li, and Douglas A. Melton

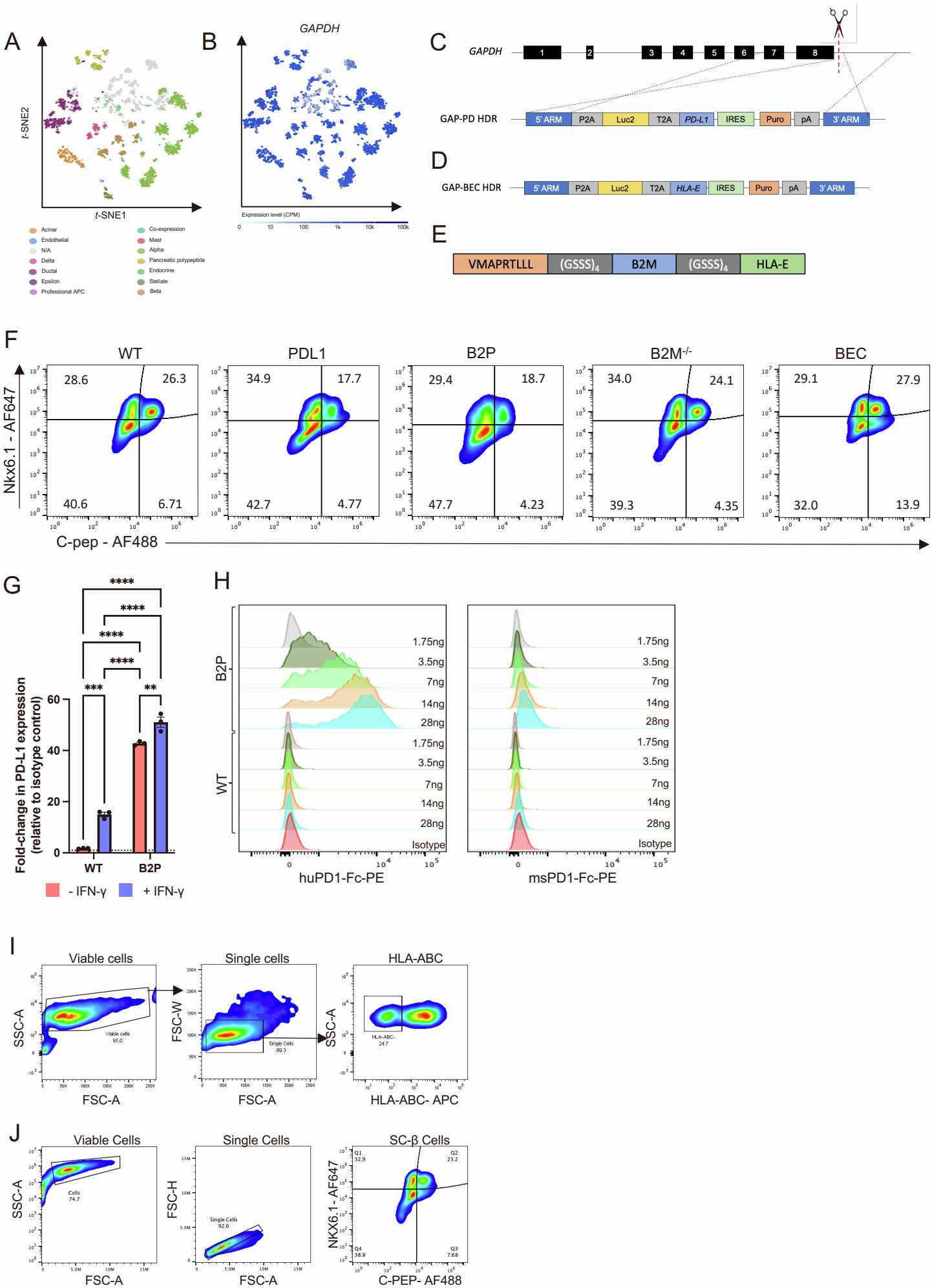
A
t-SNE2
t-SNE1
Acinar
Endothelial
N/A
Delta
Ductal
Epsilon
Professional APC
Co-expression
Mast
Alpha
Pancreatic polypeptide
Endocrine
Stellate
Beta
B
GAPDH
Expression level (CPM)
0
10
100
1k
10k
100k
C
GAPDH
1
2
3
4
5
6
7
8
GAP-PD HDR
5' ARM
P2A
Luc2
T2A
PD-L1
IRES
Puro
pA
3' ARM
D
GAP-BEC HDR
5' ARM
P2A
Luc2
T2A
HLA-E
IRES
Puro
pA
3' ARM
E
VMAPRTLLL
(GSSS)4
B2M
(GSSS)4
HLA-E
F
WT
PDL1
B2P
B2M-/-
BEC
28.6
26.3
40.6
6.71
34.9
17.7
42.7
4.77
29.4
18.7
47.7
4.23
34.0
24.1
39.3
4.35
29.1
27.9
32.0
13.9
Nkx6.1 - AF647
C-pep - AF488
G
Fold-change in PD-L1 expression (relative to isotype control)
WT
B2P
- IFN-γ
+ IFN-γ
****
****
****
****
***
**
H
B2P
WT
1.75ng
3.5ng
7ng
14ng
28ng
Isotype
huPD1-Fc-PE
msPD1-Fc-PE
I
Viable cells
Single cells
HLA-ABC
SSC-A
FSC-A
FSC-W
HLA-ABC- APC
Viable cells 95.0
Single Cells 89.3
HLA-ABC- 24.7
J
Viable Cells
Single Cells
SC-β Cells
SSC-A
FSC-A
FSC-H
NKX6.1 - AF647
C-PEP- AF488
Cells 74.7
Single Cells 92.6
Q1 32.9
Q2 23.2
Q4 38.8
Q3 7.68

Figure S1. Characterization of genetically-engineered hESCs and their islet derivatives. Related to Figure 1

A. t-SNE projections of primary human islet cells.
B. t-SNE projections of GAPDH expression across the assigned populations. Cells are colored according to their assigned cluster. (Adapted from Segerstolpe et al., 2016)
C. Schematic of homology directed repair plasmids for integration of Luc2 and PD-L1 at the GAPDH locus.
D. Schematic GAPDH-targeting Luc2 and peptide::B2M::HLA-E HDR plasmid.
E. Schematic of the peptide::B2M::HLA-E long-chain fusion.
F. FACS analysis of Nkx6.1^{+}/C-peptide^{+} SC-β cells derived from hypoimmunogenic hESCs (S6d14).
G. Quantitative analysis of surface expression of PD-L1. Data are presented as mean fold-change in MFI ± SD (n = 3 independent differentiations) normalized to isotype control (dashed line). P values were determined by two-way ANOVA, *$p < 0.05$.
H. PD1-Fc binding assay. PD-L1 and WT SC-islet cells were dissociated and stained with a 2-fold dilution series of PE-conjugated human and mouse PD1-Fc. Data are presented as MFI normalized to mode.
I. FACS sorting strategy of HLA-ABC$^{-/-}$ hESCs.
J. FACS gating strategy for quantification of Nkx6.1^{+}/C-pep^{+} SC-β cells following *in vitro* differentiation.

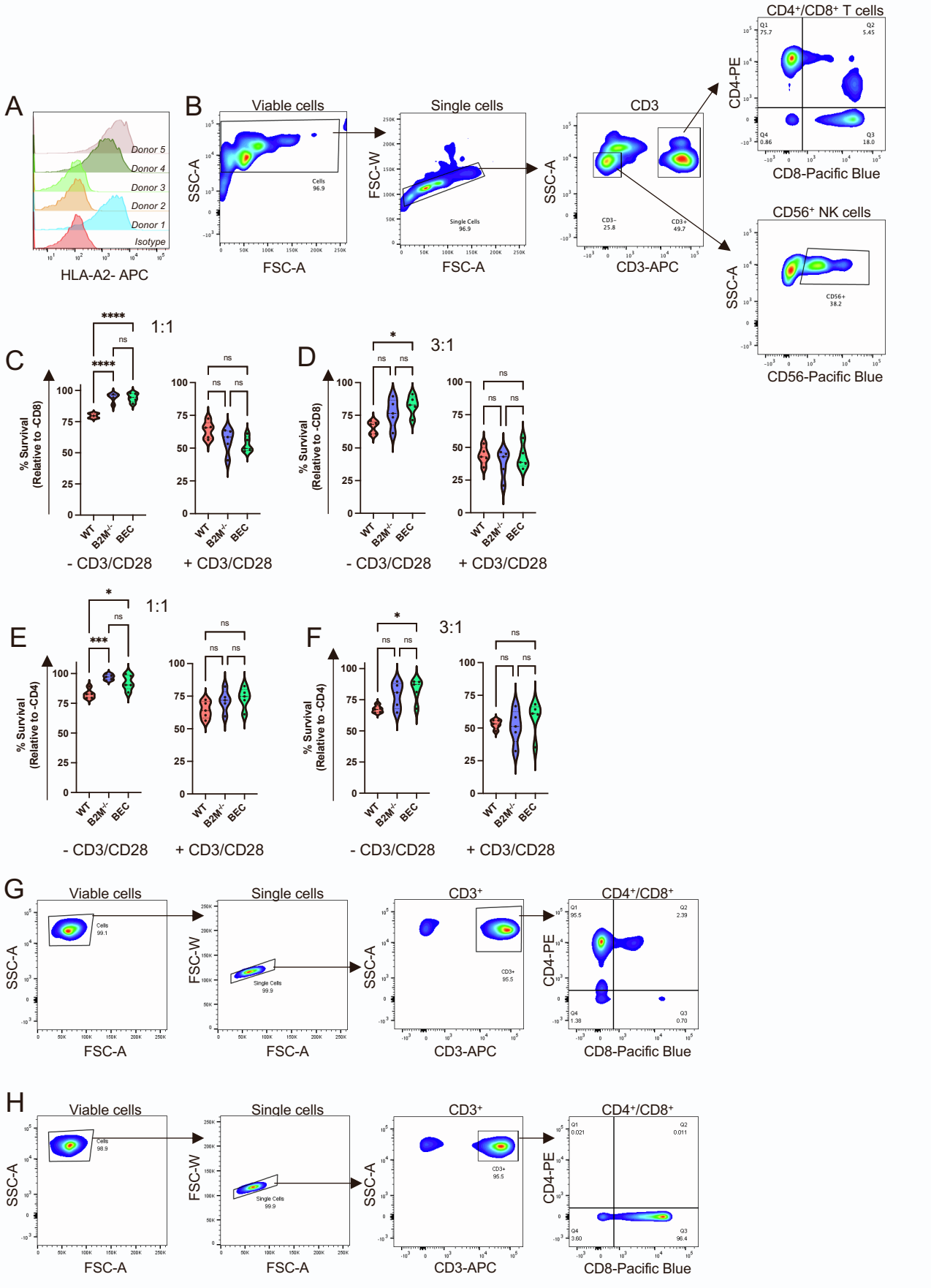
A
Donor 5
Donor 4
Donor 3
Donor 2
Donor 1
Isotype
HLA-A2- APC
B
Viable cells
SSC-A
FSC-A
Cells
96.9
Single cells
FSC-W
FSC-A
Single Cells
96.9
CD3
SSC-A
CD3-APC
CD3-
25.8
CD3+
49.7
CD4+/CD8+ T cells
CD4-PE
CD8-Pacific Blue
Q1
75.7
Q2
5.45
Q4
0.86
Q3
18.0
CD56+ NK cells
SSC-A
CD56-Pacific Blue
CD56+
38.2
C
1:1
% Survival
(Relative to -CD8)
WT
B2M-/-
BEC
- CD3/CD28
+ CD3/CD28
D
3:1
E
1:1
% Survival
(Relative to -CD4)
F
3:1
G
Viable cells
Cells
99.1
Single cells
Single Cells
99.9
CD3+
CD3+
95.5
CD4+/CD8+
Q1
95.5
Q2
2.39
Q4
1.38
Q3
0.70
H
Viable cells
Cells
98.9
Single cells
Single Cells
99.9
CD3+
CD3+
95.5
CD4+/CD8+
Q1
0.021
Q2
0.011
Q4
3.60
Q3
96.4

Figure S2: Characterization of immune subsets within human PBMCs. Related to Figure 2.

A. FACS profiling of HLA-A2 status of 5 PBMC donors.
B. FACS gating strategy of $CD4^+$ and $CD8^+$ T cells and $CD56^+$ NK cells in PBMCs enriched from human apheresis leukoreductions. Plots are representative of 5 donors.
C. Quantification of SC-islet cell survival when co-cultured with purified human $CD8^+$ T cells at a 1:1 ratio. Cell survival is presented as mean ± SD (n = 5 donors in technical triplicate). P values were determined by one-way ANOVA with Tukey's post-hoc test, $*p < 0.05$.
D. Quantification of SC-islet cell survival when co-cultured with purified human $CD8^+$ T cells at a 3:1 ratio. Cell survival is presented as mean ± SD (n = 5 donors in technical triplicate). P values were determined by one-way ANOVA with Tukey's post-hoc test, $*p < 0.05$.
E. Quantification of SC-islet cell survival when co-cultured with purified human $CD4^+$ T cells at a 1:1 ratio. Cell survival is presented as mean ± SD (n = 5 donors in technical triplicate). P values were determined by one-way ANOVA with Tukey's post-hoc test, $*p < 0.05$.
F. Quantification of SC-islet cell survival when co-cultured with purified human $CD4^+$ T cells at a 3:1 ratio. Cell survival is presented as mean ± SD (n = 5 donors in technical triplicate). P values were determined by one-way ANOVA with Tukey's post-hoc test, $*p < 0.05$.
G. FACS gating strategy of $CD4^+$ T cells enriched from human apheresis leukoreductions. Plots are representative of 5 donors.
H. FACS gating strategy of $CD8^+$ T cells enriched from human apheresis leukoreductions. Plots are representative of 5 donors.
I. FACS gating strategy of $CD56^+$ NK cells enriched from human apheresis leukoreductions. Gates for specific population include all $CD56^+$ NK cells (red), $CD56^{high}$ (green) and $CD56^{dim}$ (pink). Plots are representative of 5 donors.
J. *In vivo* NK cell assay. Scid/beige mice (n = 5) were transplanted subcutaneously with 2.5×10^5 WT or $B2M^{-/-}$ SC-islet cells in the presence or absence of a 3:1 effector:target ratio of rhIL-2 pre-treated primary human NK cells. Bioluminescence imaging was performed on day 1 and 5 post-transplantation.

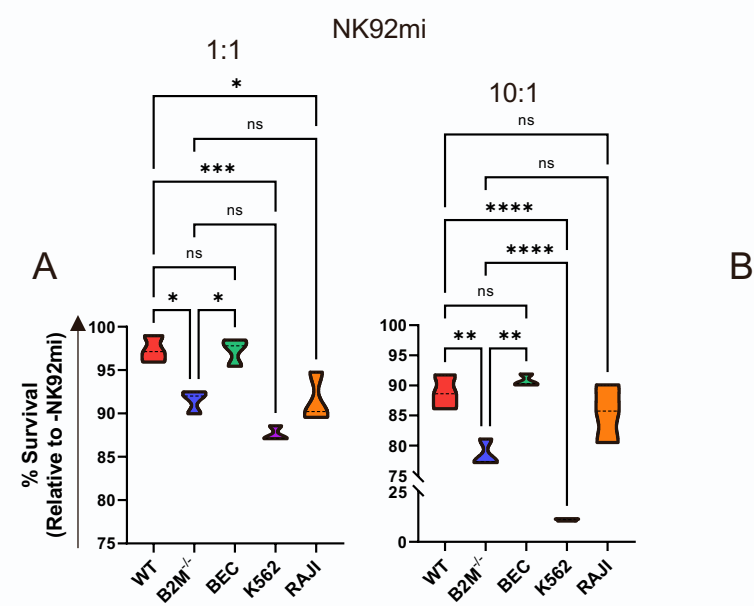
NK92mi
1:1
10:1
A
% Survival
(Relative to -NK92mi)
WT
B2M-/-
BEC
K562
RAJI
*
ns
***
****
**

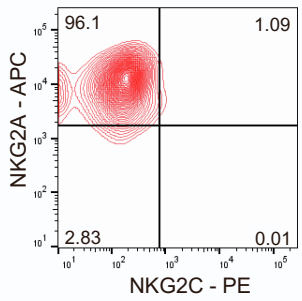
B
96.1
1.09
2.83
0.01
NKG2A - APC
NKG2C - PE

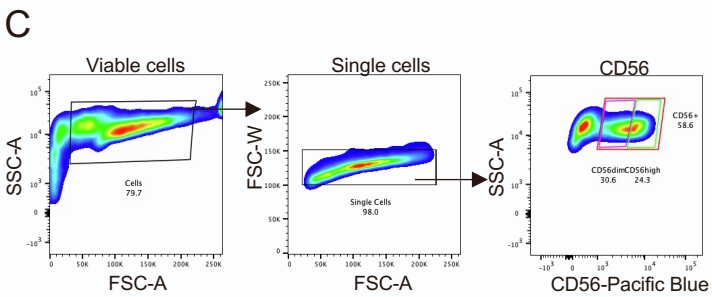
C
Viable cells
Single cells
CD56
SSC-A
FSC-A
FSC-W
CD56-Pacific Blue
Cells
79.7
Single Cells
98.0
CD56+
58.6
CD56dimCD56high
30.6
24.3

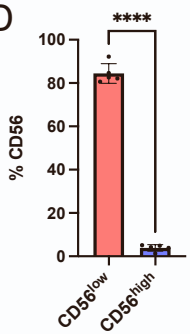
D
****
% CD56
CD56low
CD56high

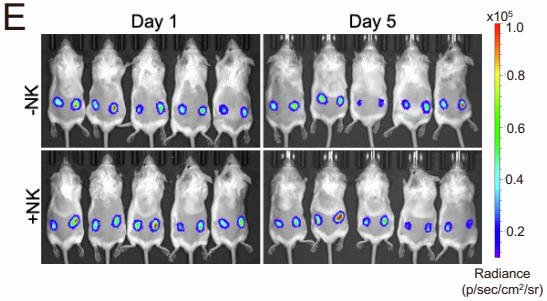
E
Day 1
Day 5
-NK
+NK
x10^5
Radiance
(p/sec/cm²/sr)

Figure S3: *In vitro* and *in vivo* co-culture of hypoimmunogenic SC-islet cells with primary and immortalized human NK cells. Related to Figure 3.

A. Quantification of SC-β cell survival when co-cultured with NK92mi cells at 1:1 and 10:1 NK:SC-β cell ratios. K562 and Raji cells were used as positive and negative controls, respectively. Cell survival is presented as mean ± SD (n = 5 donors in technical triplicate).
B. NKG2A/NKG2C expression on NK92mi cells.
C. FACS gating strategy of $CD56^{+}$ NK cells enriched from human apheresis leukoreductions. Gates for specific population include all $CD56^{+}$ NK cells (red), $CD56^{high}$ (green) and $CD56^{dim}$ (pink). Plots are representative of 5 donors.
D. Quantitative analysis of CD56 expression on enriched primary human NK cells. Data is presented as % CD56 expression (n = 5 donors in technical triplicate).
E. *In vivo* NK cell assay. Bioluminescence imaging was performed on day 1 and 5 post-transplantation.

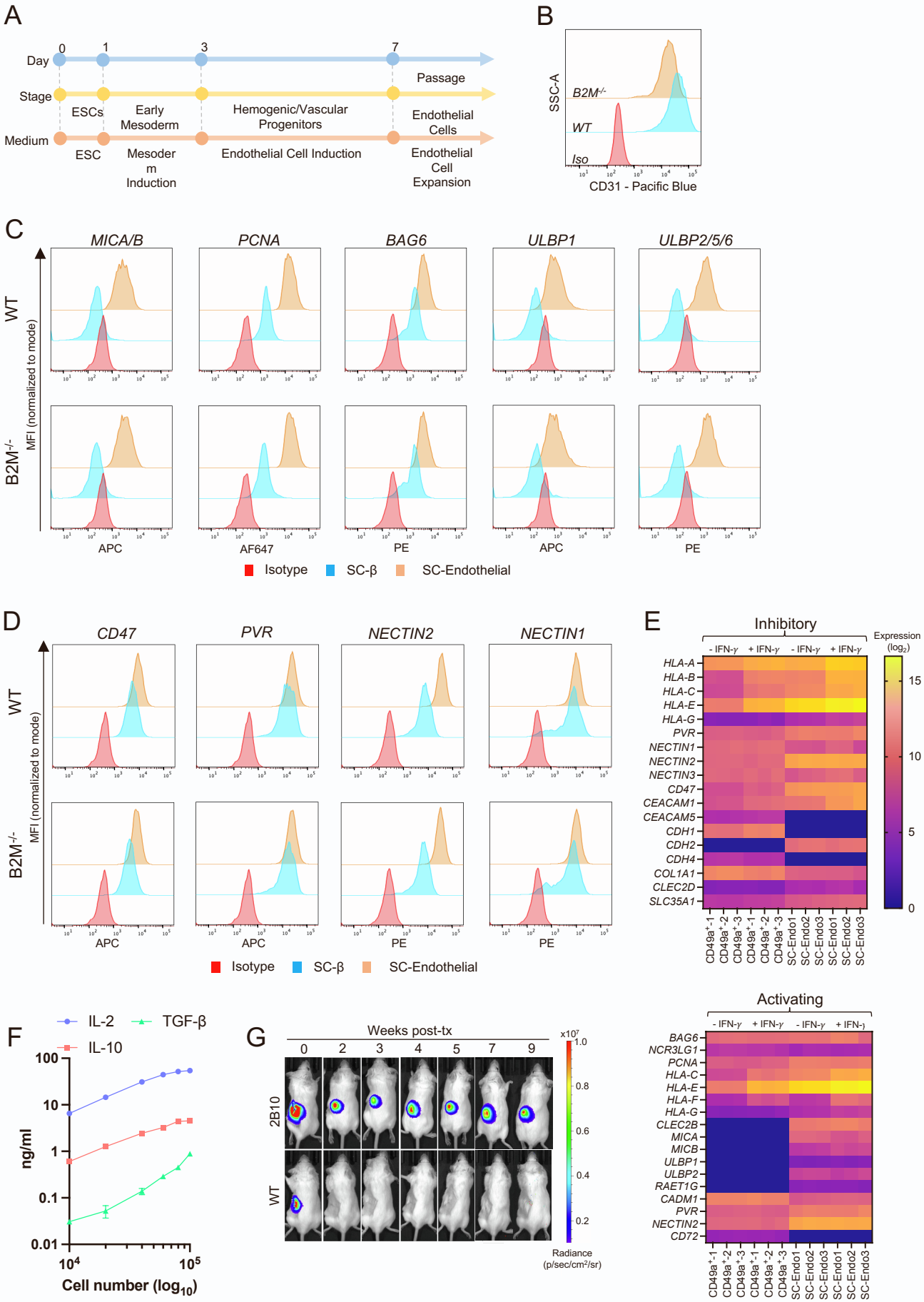
A
Day
Stage
Medium
0
1
3
7
ESCs
ESC
Early Mesoderm
Mesoderm Induction
Hemogenic/Vascular Progenitors
Endothelial Cell Induction
Passage
Endothelial Cells
Endothelial Cell Expansion
B
SSC-A
B2M-/-
WT
Iso
CD31 - Pacific Blue
C
MICA/B
PCNA
BAG6
ULBP1
ULBP2/5/6
WT
B2M-/-
MFI (normalized to mode)
APC
AF647
PE
APC
PE
Isotype
SC-β
SC-Endothelial
D
CD47
PVR
NECTIN2
NECTIN1
WT
B2M-/-
MFI (normalized to mode)
APC
APC
PE
PE
Isotype
SC-β
SC-Endothelial
E
Inhibitory
- IFN-γ
+ IFN-γ
- IFN-γ
+ IFN-γ
Expression (log2)
HLA-A
HLA-B
HLA-C
HLA-E
HLA-G
PVR
NECTIN1
NECTIN2
NECTIN3
CD47
CEACAM1
CEACAM5
CDH1
CDH2
CDH4
COL1A1
CLEC2D
SLC35A1
CD49a+-1
CD49a+-2
CD49a+-3
CD49a--1
CD49a+-2
CD49a+-3
SC-Endo1
SC-Endo2
SC-Endo3
SC-Endo1
SC-Endo2
SC-Endo3
Activating
BAG6
NCR3LG1
PCNA
HLA-C
HLA-E
HLA-F
HLA-G
CLEC2B
MICA
MICB
ULBP1
ULBP2
RAET1G
CADM1
PVR
NECTIN2
CD72
F
IL-2
TGF-β
IL-10
ng/ml
Cell number (log10)
G
Weeks post-tx
0
2
3
4
5
7
9
2B10
WT
x10^7
Radiance (p/sec/cm²/sr)

Figure S4: Characterization of the NK cell ligand profile on SC-islet and SC-endothelial cells. Related to Figures 3 and 4.

A. Schematic of SC-endothelial cell differentiation protocol.
B. FACS analysis of the endothelial cell marker CD31 in SC-endothelial cells derived from WT and B2M$^{-/-}$ hESCs.
C. NK cell activating ligand expression on SC-β and SC-Endothelial cells. Data are presented as MFI normalized to mode and is representative of three independent experiments.
D. NK cell inhibitory ligand expression on SC-β and SC-Endothelial cells. Data are presented as MFI normalized to mode and is representative of three independent experiments.
E. Heatmap of NK cell ligand expression in SC-β and SC-Endothelial cells (-IFN-γ vs +IFN-γ). Ligand expression is presented as fold-change (log_2).
F. Quantification of cytokine secretion from 2B10 SC-islet cells. Data are presented as mean ± SD (n = 2).
G. *In vivo* bioluminescence imaging of B6/albino mice transplanted with WT and 2B10 SC-islet cells (n = 3/group).